General Disclaimer

One or more of the Following Statements may affect this Document

- This document has been reproduced from the best copy furnished by the organizational source. It is being released in the interest of making available as much information as possible.

- This document may contain data, which exceeds the sheet parameters. It was furnished in this condition by the organizational source and is the best copy available.

- This document may contain tone-on-tone or color graphs, charts and/or pictures, which have been reproduced in black and white.

- This document is paginated as submitted by the original source.

- Portions of this document are not fully legible due to the historical nature of some of the material. However, it is the best reproduction available from the original submission.

NATIONAL AERONAUTICS AND SPACE ADMINISTRATION

Technical Memorandum 33-616

The Mariner 9 Power Subsystem Design and Flight Performance

Robert H. Josephs

JET PROPULSION LABORATORY
CALIFORNIA INSTITUTE OF TECHNOLOGY
PASADENA, CALIFORNIA

May 15, 1973

NATIONAL AERONAUTICS AND SPACE ADMINISTRATION

Technical Memorandum 33-616

The Mariner 9 Power Subsystem Design and Flight Performance

Robert H. Josephs

JET PROPULSION LABORATORY
CALIFORNIA INSTITUTE OF TECHNOLOGY
PASADENA, CALIFORNIA

May 15, 1973

PREFACE

The work described in this report was performed by the Guidance and Control Division of the Jet Propulsion Laboratory.

TABLE OF CONTENTS

LIST OF ILLUSTRATIONS

LIST OF ILLUSTRATIONS (contd)

LIST OF TABLES

ACKNOWLEDGMENT

The author wishes to thank L.A. Packard for his valuable assistance in the preparation of this report. The author is also grateful for the counsel of P. Wiener, supervisor of the Power Systems and Programs Group at the Jet Propulsion Laboratory.

ABSTRACT

This report documents the design and flight performance of the Mariner Mars 1971 power subsystem. Mariner 9 was the first spacecraft to orbit another planet, and this report discusses some of the power management techniques employed to support an orbital mission far from earth with marginal sunlight for its photovoltaic-battery power source. It also describes the performance of its nickel-cadmium battery during repetitive sun occultation phases of the mission, and the results of unique tests in flight to assess the performance capability of its solar array.

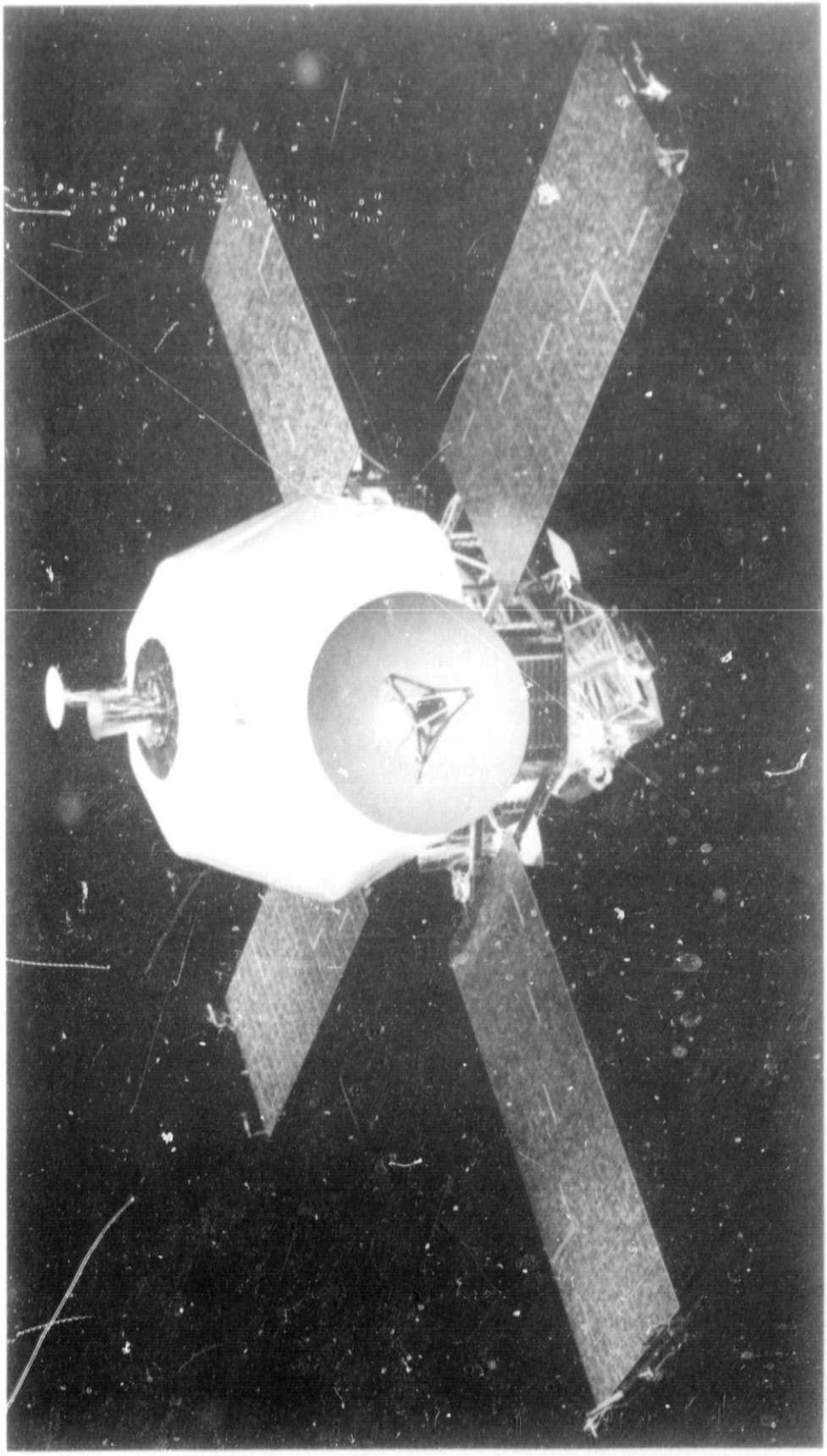

Frontispiece. Mariner Mars 1971 Orbiter

SECTION 1

MARINER MARS 1971 POWER SUBSYSTEM DESIGN

1.1 INTRODUCTION

The design goal for the MM'71 was to build a suitable power supply which retained as much of the MM'69 design as possible. However, past Mariner programs had been planet fly-bys. MM'71 was the first orbit of mission to another planet, and as such, this Mariner mission required some departure from previous Mariner power subsystem design, particularly with regard to the battery. The following is a functional description of the MM'71 power subsystem, followed by a discussion of its design and design changes from prior programs, and a review of its flight performance.

1.2 MM'71 POWER SUBSYSTEM FUNCTIONAL DESCRIPTION

As with Mariner spacecraft to date, the primary spacecraft electrical power was derived from energy converted from sunlight by solar panels. The solar panels were stowed parallel to the thrust axis of the launch vehicle, and pyrotechnic devices were timed on board to release them during the launch sequence. The spring loaded panels deployed 90 degrees to lock into a position perpendicular to the spacecraft roll axis, after which automatic spacecraft attitude control maintained the array within 0.25 deg of the Sun vector during normal mission operation. See Frontispiece.

A 20 ampere-hour nickel-cadmium rechargeable battery supported the electrical power requirements of the spacecraft during launch, and thereafter whenever spacecraft loads exceeded available array power. The battery was maintained near full charge at every opportunity during the mission to have the battery at its optimum charge state in the event of sudden unexpected need. Battery charging was provided by a charger with two rates, high rate at 2.0 amperes (C/10), and low rate at 0.65 amperes (C/30). High rate was designed to recharge the battery most efficiently in a short time interval. The low or trickle charge rate maintained the battery at full capacity when the battery was not being used, as it replenished the battery capacity lost through normal self-discharge of the nickel-cadmium battery system.

Unregulated DC power on MM'71, at a potential range of 27 to 50 VDC, supported the operation of the TWTA power converter, DC heaters, 30 VDC regulator, and the battery charger. The MM'71 Power Subsystem Functional Block Diagram is shown in Figure 1-1. About one-third of the MM'69 spacecraft electrical power was used directly from the unregulated bus. Unregulated DC spacecraft loads varied during the MM'71 mission, a function of the spacecraft heliocentric distance, and reached 51% of the total spacecraft loads during cruise just prior to Mars orbit insertion. However, with the science loads coming on after orbit insertion, and the DC replacement heaters having turned off, the ratio of MM'71 unregulated DC power to the total spacecraft power requirements reduced to about 28%. The balance of the output of the unregulated DC power bus was routed to the booster regulator, that boosted and regulated to 56 VDC ± 1% at the output.

The regulated DC output of the booster regulator was not directly used by the MM'69 and MM'71 spacecraft. The science instruments and most of the MM'71 engineering subsystems were AC powered either at 400 Hz, or at 2.4 kHz. A 400 Hz three phase inverter provided three phase, quasi-square wave power to the three gyroscope spin motors. The science scan platform position was controlled by two single phase motors using 28 Vrms square wave power provided by a single phase 400 Hz inverter, while the science instruments and the remaining subsystems were powered by a 50 Vrms square wave, 2.4 kHz inverter. The function of the booster regulator was to power these three inverters. Spacecraft events were timed by the MM'71 central computer and sequencer (CC&S) clock, the frequency reference for which was the 2.4 kHz ± 0.01% frequency output of the main inverter. Both 400 Hz inverters were also synchronized by the main inverter, and had the same nominal frequency tolerance of ± 0.01%. The 2.4 kHz inverter operated continuously during the MM'71 mission from the time spacecraft power was powered on the launch pad, while the 400 Hz inverters were turned on during the mission as needed.

1.3 MM'71 POWER SUBSYSTEM DESIGN

The following discusses the MM'71 power subsystem design and stresses significant changes from the design used on MM'69. The Mariner 9 power subsystem supported, in flight, the power profile shown in Figure 1-2.

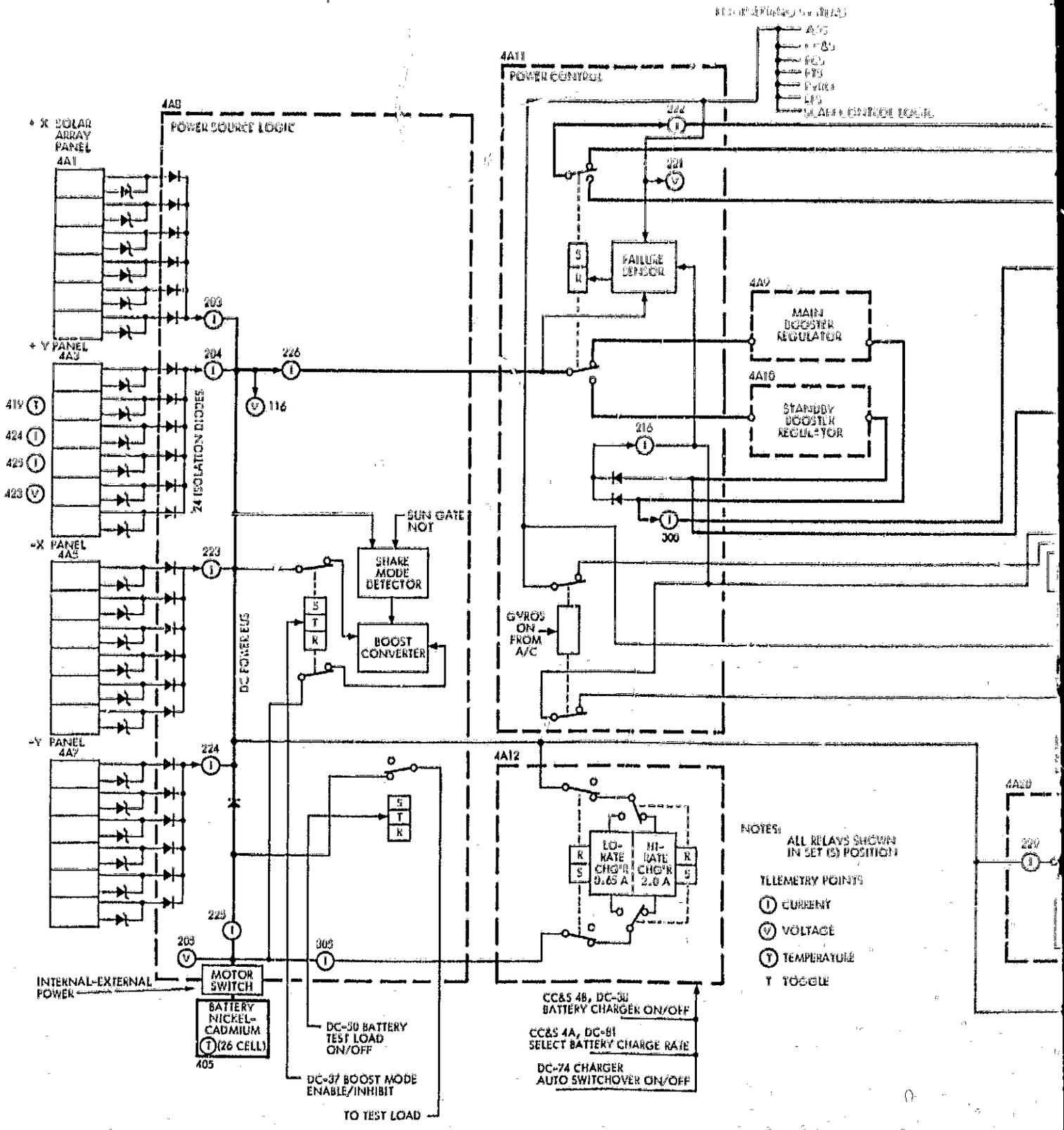

FOLDOUT FRAME 1

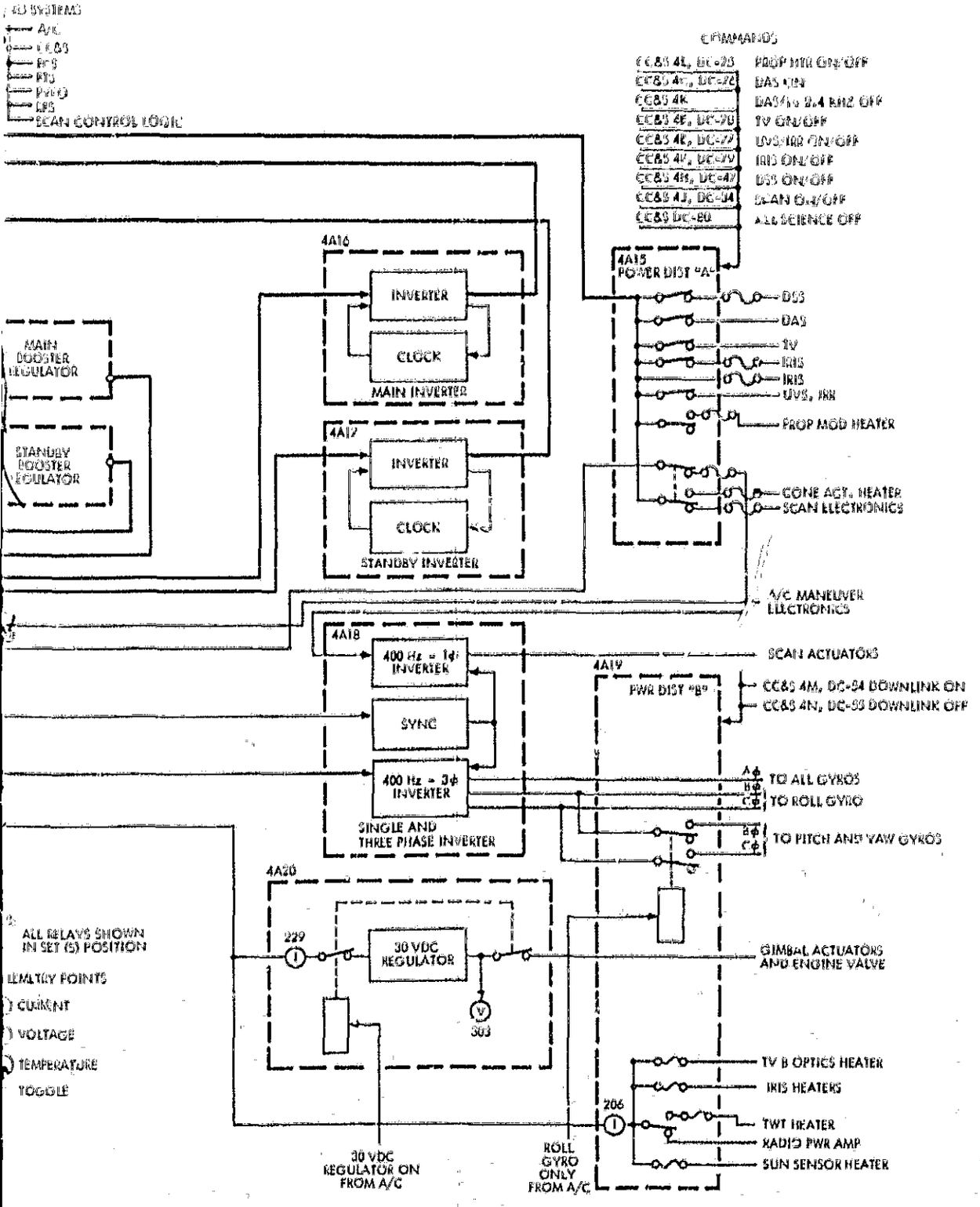

Figure 1-1. MM'71 Power Subsystem Functional Block Diagram

FOLDOUT FRAME 2

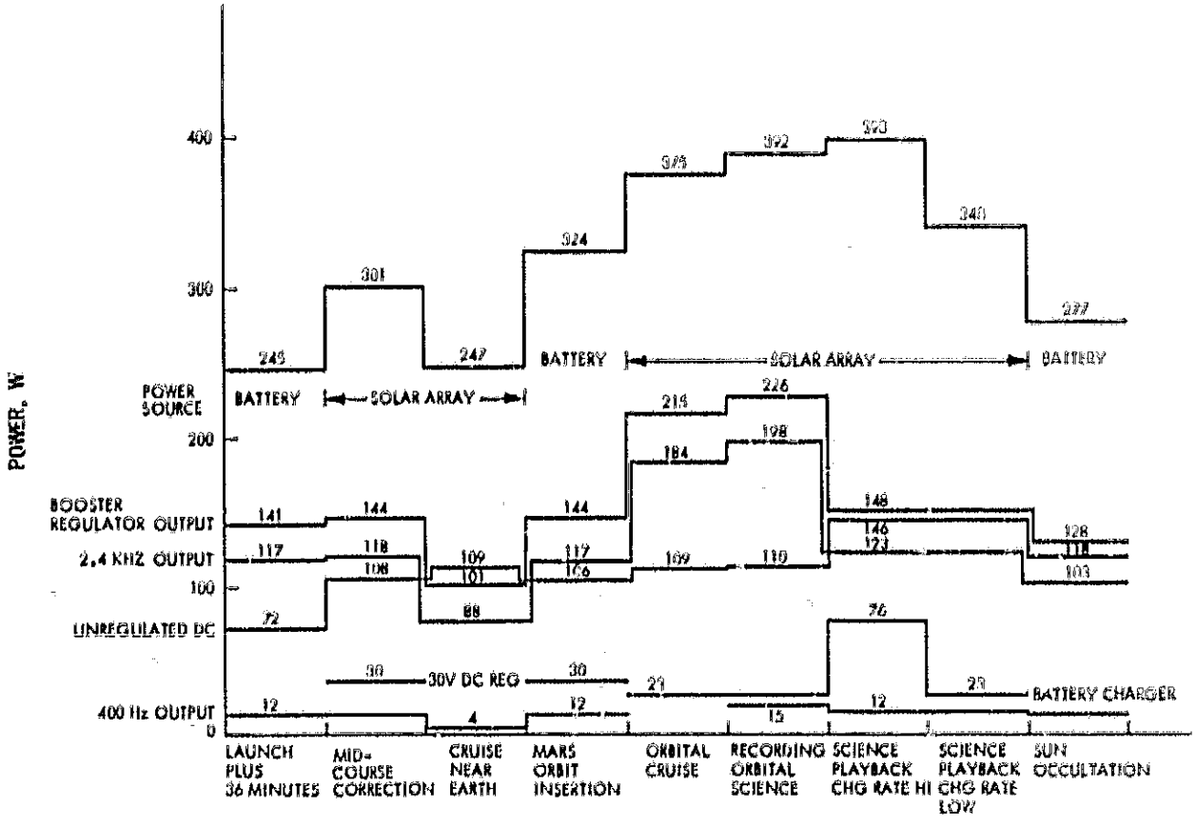

Figure 1-2. Mariner Mars 1971 Mission Power Profile

Table 1-1 tabulates some of the MM'71 power subsystem parameters.

a. Solar Array. The MM'71 solar array circuit arrangement was the same as that used for MM'69. Solar panel temperature sensors were reduced from two on MM'69 to one on MM'71, and outriggers were used to mechanically extend the solar panel structures from the spacecraft bus. The extension provided clearance between the stowed panels and the larger propulsion fuel tanks used on MM'71, and clearance for the high gain antenna. In all other respects, the MM'69 and MM'71 solar panel designs were identical, see Figure 1-3 and 1-4.

Each of the four solar panels was 0.9 m (35.5 in.) by 2.14 m (84.3 in.) with an area of 1.93 m^2 (20.8 ft^2) or about 7.7 m^2 (83 ft^2) for the array. Solar cells used were 2 x 2 cm N/P, 1 to 3 ohm-cm base resistivity, 0.457 mm (18 mils) thick, that had silver-over-titanium vacuum deposited contacts that were solder coated. The cell material was phosphorous-diffused, boron doped silicon. A total of 4,368 solar cells were bonded to each of the four solar panels, and were insulated from the aluminum substrate by a dielectric consisting of Epon 956 epoxy adhesive impregnated sheet fiberglass. There were 78 cells connected in series, and 224 cells connected in parallel on the total array.

The optically coated solar cell coverglass was 7094 fused silica 0.508 mm (20 mils) thick, each of which was bonded to a solar cell surface with RTV 602 transparant adhesive. Each of the 24 submodule sections that comprised the total array was diode isolated from the DC power bus to prevent an electrical fault within any one

Table 1-1. Mariner 9 Power Subsystem Parameters

Solar Array Maximum Power	
Predicted at encounter, 67 mw/cm^2, 30°C	42[illegible] w
Performance at encounter, 67 mw/cm^2, 24°C, 4[illegible] degradation	412 w*
Battery	
Potential	27.[illegible] VDC
Rated Capacity	20 amp-hr
Performance Capacity	2[illegible] amp-hr*
DC Power Bus Potential	25.50 VDC
Battery Charger	
High Rate Charge,	2.03 amps*
@ Charger Potential Drop of 4 V	
Low Rate Charge,	0.[illegible]3 amp*
@ Charger Potential Drop of 8.9 volts*	.07 6 volts*
High Rate to Low Rate Transfer Potential	
Booster Regulators	
Input Voltage	23.5-30 VDC
Output Voltage	36 VDC ±1[illegible]
Minimum Power Rating	50 w
Maximum Power Rating	298 w
24 kHz Inverters	
Input Voltage	36 VDC ±1[illegible]
Output Voltage (98-250 w output)	80 VRMS, +3[illegible], -4[illegible]
Maximum Power Rating	250 w
Frequency	2400 Hz ±0.01[illegible]
Free Running Frequency	
Main Inverter	2800 Hz ±6[illegible]
Standby Inverter	2400 Hz ±6[illegible]
400 Hz Inverters	
Single Phase	
Input Voltage	58.2 VDC ±2[illegible]
Output Voltage	28 VRMS ±6[illegible]
Average Load Rating	12 w
Peak Load Rating	18 w
Three Phase	
Input Voltage	58.2 VDC ±2[illegible]
Output Voltage	27.2 VDC ±6[illegible]
Average Load Rating	12 w
Peak Load Rating (60 seconds)	18 w
30 Volt DC Regulator	
Input Voltage	28-50 VDC
Output Voltage	30 VDC ±8[illegible]
Minimum Power Rating	12 w
Maximum Continuous Power Rating	60 w
Maximum (90 minutes)	90 w
Peak (60 seconds)	150 w
Boost Converter	
with E_{IN} at 26V @ E_{OUT} 34V, I_{OUT} 8 ma	
with E_{IN} at 26V @ I_{OUT} 4.8a, E_{OUT} = 25 ±1 volt	
with I_{IN} at 33V @ E_{OUT} 50V, I_{OUT} 4ma	
Pulse Duration: 0.6 second	
Repetition Rate: 7.5 seconds	

*Flight or Test Data

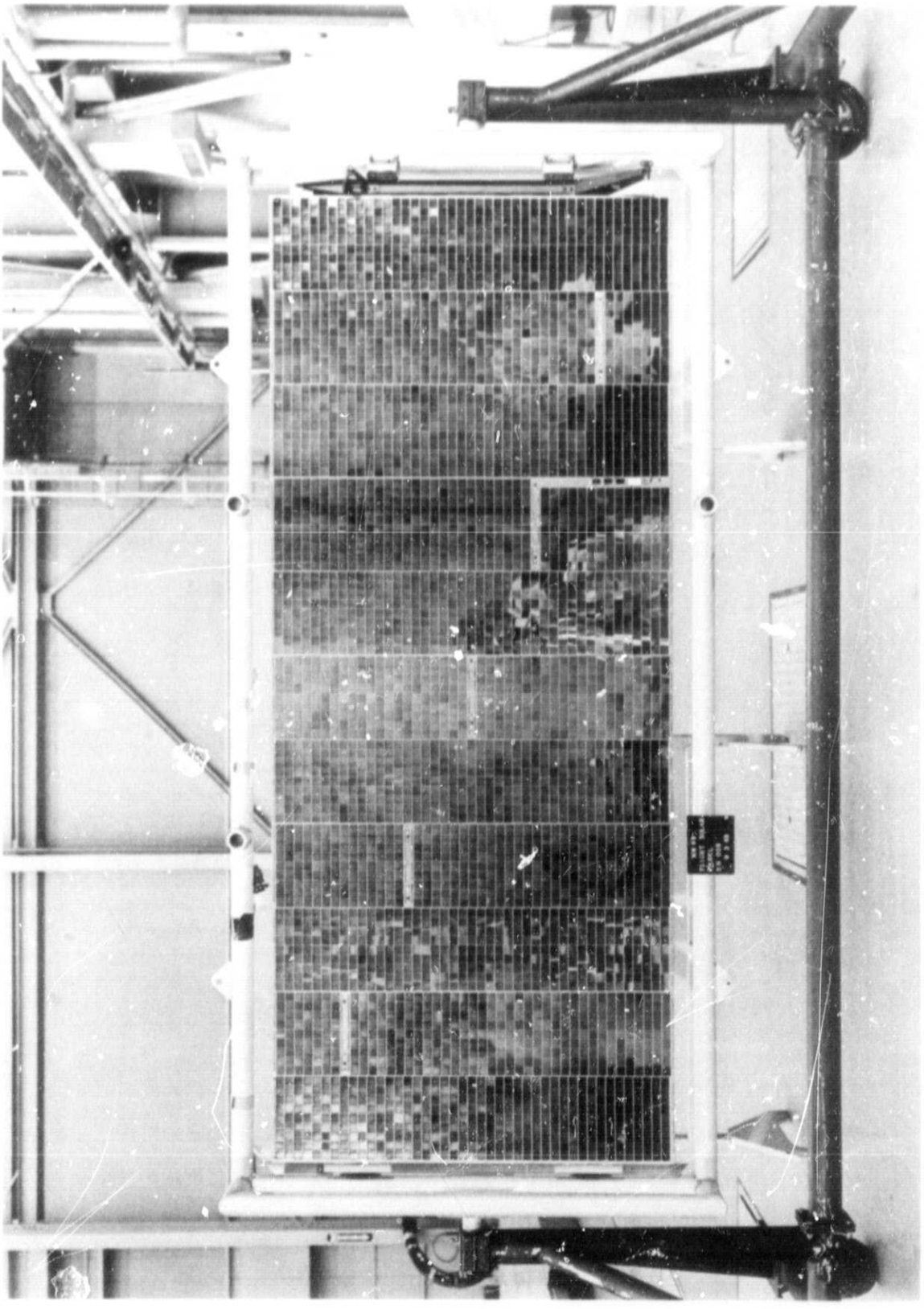

Figure 1-3. The MM'69 Solar Panel Design Used on Mariner Mars '71, Front

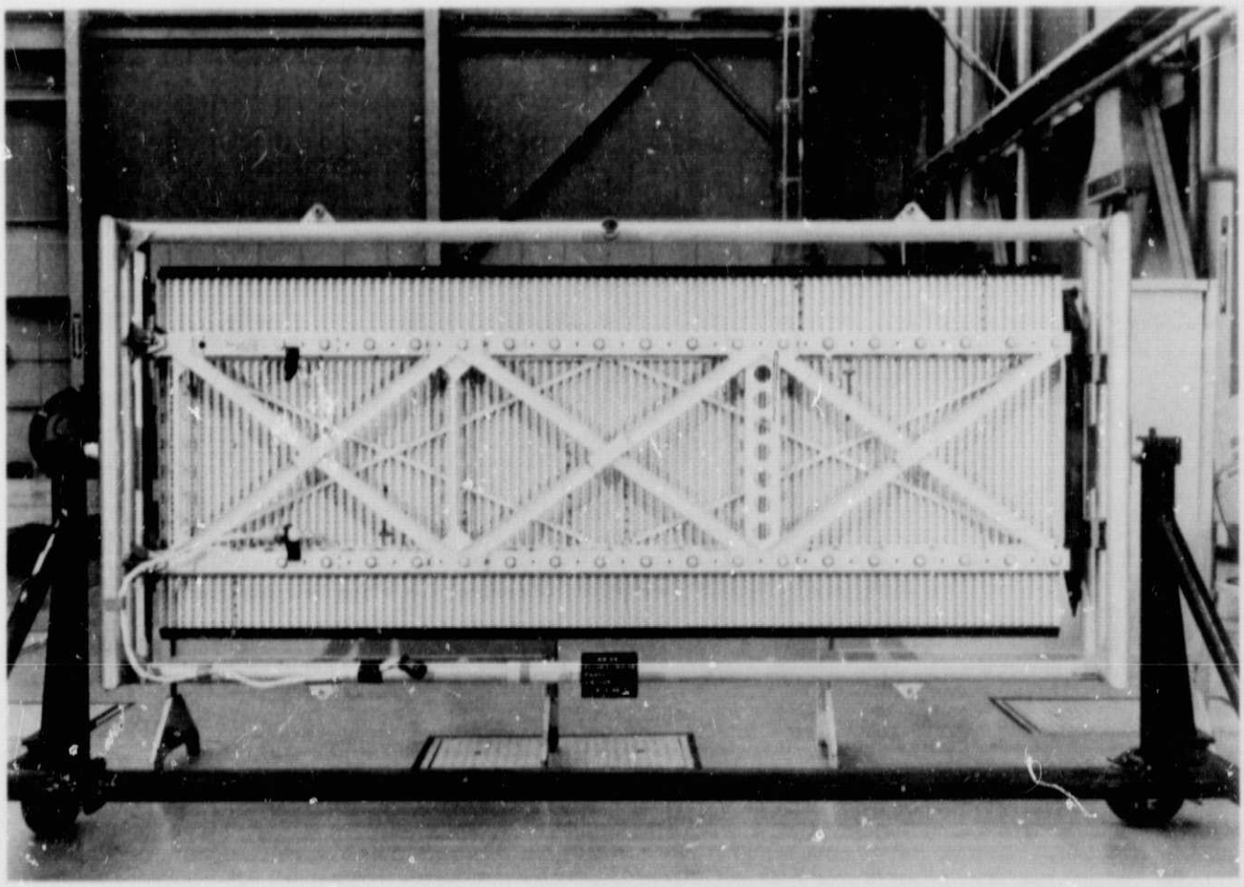

Figure 1-4. The MM'69 Solar Panel Design Used on Mariner Mars '71, Rear

section from seriously affecting the total array output. The isolation diodes were physically located in the power source logic module of the PCE. Six series connected zener diodes also shunted each of the 24 submodule sections. The zeners were stud mounted upon spars on the rear of each solar panel facing deep space, Figure 1-4, and had a voltage temperature coefficient of +2.99 mV/°C. The solar array could operate at high potentials when cold, that would interfere with the performance of the booster regulator. Because the booster regulator was not designed to operate at input potentials that were higher than its output, the array zeners were designed to limit array potentials below 50 Volts when the array was cold, as it was after emerging from solar occult sequences, or after the spacecraft had receded sufficiently far from the Sun.

As with previous Mariner array designs, MM'71 incorporates into the array three solar cell transducers to provide telemetered engineering data. The cells are 1 x 2 cm because of mounting area limitations, but are otherwise typical of those used for the array, including coverglass and adhesive. Precision resistor loads are selected for these cells to measure the short circuit current of two cells and the open circuit voltage of the third, and to provide proper input to the spacecraft telemetry system. The short circuit current of one of the I_{sc} cells on the Mariner 9 had been deliberately degraded 42.8% by electron bombardment of 3×10^{16} e/cm^2 at 1 MeV. In this manner, the irradiated I_{sc} cell was rendered relatively insensitive to further radiation damage in space, and its telemetered output could be compared to that of the I_{sc} cell that was still radiation sensitive. The objective was to provide an index for radiative flux that could damage the array.

More detailed discussion of the design and operation of the MM'71 solar array, and other power subsystem components that were relatively unchanged from

MM'69 designs, may be found in the Mariner Mars 1969 Final Project Report: Development, Design and Test, Volume 1, JPL Technical Report 32-1460, 1 November 1970, p. 373 ff.

b. Battery. The major modification from the MM'69 power subsystem design was the new MM'71 nickel-cadmium battery. A 20 ampere-hour 26 cell Ni-Cd battery replaced the 18 cell 50 ampere-hour silver-zinc battery used on MM'69, essentially because of the orbital nature of MM'71. In addition to the use of the battery at launch, midcourse maneuver, and standby at planet encounter, as Mariner battery mission requirements had been for prior programs, the MM'71 battery had critical spacecraft support requirements for the Mars orbit insertion and trim maneuvers after a 5-1/2 month cruise interval had elapsed. This required a battery with greater cycle reliability than the Ag-Zn. The Ni-Cd also permitted spacecraft survival through MM'71 post-mission intervals having orbital Sun occultations, and unlike Ag-Zn, it placed no constraint upon the accumulated number of cycles that may be used for science gathering or playback. Figure 1-5 shows the Mariner '71 battery, and its side view in Figure 1-6 shows the wiring to the individual battery cells.

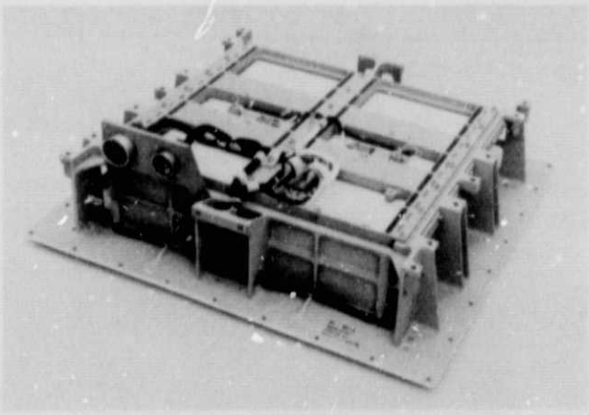

Figure 1-5. MM'71 Nickel Cadmium Battery

c. Power Conditioning. MM'69 power conditioning equipment (PCE) was somewhat modified to accommodate greater power requirements of the MM'71 mission. It was also modified to provide more complex switching and power distribution. The following discusses the design of the MM'71 PCE and again flags significant modifications of the MM'69 design.

d. Battery Charger. The MM'69 battery charger was a current limited series regulator, whose charge rate varied

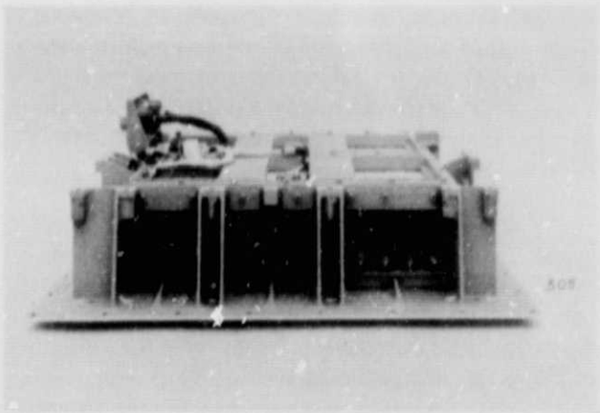

Figure 1-6. Side View of Nickel-Cadmium Battery

from 10 to 650 mA depending upon the relative potentials at the DC power bus and battery. The MM'71 charger for the Ni-Cd was a more sophisticated device with two charge rates. A high rate mode at 2.0 amperes was provided by a pulse-width modulated switching regulator. Constant current regulation in the high rate charger was maintained by duty-cycle variation of the series regulator as a function of output current changes. A low charge rate was provided by a constant current series regulator whose fixed output at about 0.6 ampere was controlled by the voltage developed across a resistor in series with its output. The output current of both chargers was further influenced by the relative potentials of the DC power bus and the battery. The MM'71 battery charger circuitry automatically transferred the high charge rate mode to low charge rate at times when:

1) The battery was near full charge. As the battery terminal voltage reached 37.5 volts, the charger voltage detection circuit sensed the battery approaching full charge, and automatically caused the charger to switch to low rate, in which charge mode the battery recharge sequence was completed. This was the usual charge sequence during the mission.

2) The battery reached high temperatures. Automatic transfer from the high to the low charge rate mode was also effected should the battery temperature approach 37.8°C (100°F). This condition never occurred during the mission.

Battery charger commands were issued either by the direct ground command system, or by commands

stored in the central computer and sequencer. The commands toggled the unit on or off, or changed the charge rate mode. Timed high rate charge sequences were possible when the charger's automatic voltage detection circuit was inhibited, and the charge rate mode over a desired time interval was selected by command.

Charger Lockup. The Mariner 9 battery was recharged at high rate only after the discharge exceeded 0.4 ampere-hours. This procedure insured the battery potential was below 37.5 volts when the charge was commanded into the high rate mode, after discharge, to avoid high rate charge lockup. One cause of lockup was a high rate charge command received by the charger when the battery potential was at, or exceeded, the 37.5 volt transfer potential. Whether this condition existed, or other conditions existed that could cause lockup, was carefully screened whenever the high rate command was issued. No lockup occurred during the Mariner 9 mission.

High rate lockup describes a condition of the battery charger while it was operating in its high rate mode when it could not transfer to the low rate mode. The concern was that the battery may be overcharged to permanent damage, or failure. The condition was caused by an undesired logic state caused by the simultaneous discharge of both the set and reset transfer capacitors that drive the high rate-low rate transfer relay in the unit. The discharge of one or the other capacitor through the relay coil caused state change. In lockup, the charger remained in the high rate mode until a series of ground commands restored its proper logic state, that is, until one of the transfer capacitors was recharged.

e. **30 Vdc Regulator.** The MM'71 gimbal actuators and propulsion engine valve power requirements necessitated a power source that distributed 30 Vdc to the spacecraft on the Mariner orbiter. The unit was a pulse-width modulated down regulator and a DC to DC converter with a 150 watt peak power rating at an output voltage of 30 Vdc ±5%. The power source for this module was the unregulated DC power bus, and it was switched on by a relay in the regulator that was energized by a command from the attitude control subsystem. The module provided an isolated output to the users that referenced their power returns to the spacecraft structure from which the 30 Vdc power return was isolated.

f. **Power Source and Logic.** As with past Mariner power subsystem designs, all input electrical power passed through this module, that which was generated by an external source on ground, by the solar array, or the battery. It contained the motor driven switch that transferred power at launch from the external power supply to the spacecraft battery. It also contained the quad-diode logic that automatically permitted the battery to supplement the array electrical output when the spacecraft power requirements exceeded the array output power capability, and which isolated the battery.

The MM'71 power source and logic (PS&L) also housed the share mode detector and boost converter circuitry. These circuits, that detect and relieve the power subsystem of an unnecessary battery-share mode, were located in the MM'69 battery charger module. The MM'71 PS&L also housed the battery test load relay, while for MM'69, the relay was located on the heater and DC power distribution module.

The modified PS&L in MM'71 was able to accommodate the additional circuitry because of circuitry volume reduction with welded modules that was used by a Mariner power subsystem for the first time. These modules packaged circuits that were repetitively used in the power subsystem, such as circuits for telemetry and command, and also some of the regulated supplies used for command functions. The larger unit in Figure 1-7 is a welded module that houses a relay driver used in Mariner '71 PCE. The smaller unit in Figure 1-7 is a thick film version of the same relay driver that is presently undergoing tests as a candidate for a new generation of PCE modules of greater circuitry density. Figure 1-8 shows the density of the welded module packaging in the MM'71 power distribution A subassembly.

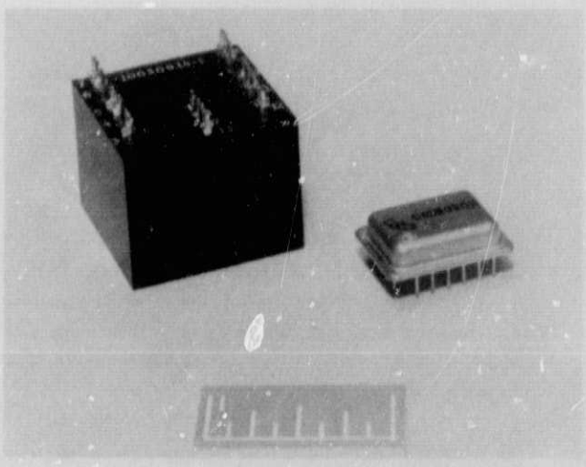

Figure 1-7. MM'71 Welded Module

Figure 1-8. MM'71 Welded Module Packaging in Power Distribution A Subassembly

g. **Other MM'71 PCE Components.** Mission requirements necessitated increasing the power rating of the MM'71 booster regulators and 2.4 kHz inverters. The booster regulator rating was increased from 250 watts for the MM'69 units to 295 watts for the units used on MM'71. The rating of the 2.4 kHz inverters was increased from 200 to 250 watts. Table 1-2 shows the maximum and minimum requirements of these units during the Mariner 9 mission. The maximum load shown is the largest electrical load supported by a Mariner power subsystem in flight. The single and three phase 400 Hz inverters were the same for both programs. Also, the redundant dual power chain philosophy used on past Mariners has been retained on MM'71, as have the share mode detector and boost converter. The function of these circuits is described in the referenced JPL TR 32-1460.

h. **MM'71 Power Distribution.** Severe power transients often accompanied MM'69 science turn on, when the mechanization to turn on the instruments required they all be switched on simultaneously. Individual science instruments were mechanized to be switched in MM'71 to make turn-on transients more manageable. It also provided for greater power management flexibility throughout the mission. Both the MM'69 power distribution, and the DC heater and power distribution modules were modified to obtain the more intricate power distribution. More efficient power utilization was also realized on MM'71 with the following modifications:

1) **Replacement Heaters.** Science instrument replacement heaters that operated from the 2.4 kHz bus on MM'69 were transferred to the unregulated DC power bus on MM'71. These are the heaters that automatically operate when the instruments are off, to maintain proper ambient temperatures. Direct operation from the DC power bus saved about 20% additional array power that would have been otherwise lost in overcoming the normal 2.4 kHz inverter and booster regulator power losses.

2) **Roll Gyro.** The MM'71 roll gyro was designed to be used independently of the pitch and yaw gyros, unlike the MM'69 mechanization that required simultaneous operation of all three gyros. Roll gyro operation was by far the predominant gyro operating mode on MM'71, and this efficient mechanization saved 10 watts at the array.

i. **MM'71 Power Subsystem Telemetry.** Table 1-3 summarizes the MM'71 power subsystem telemetry channels, and Figure 1-9 locates each in a simplified power subsystem functional diagram. In addition to those listed, telemetry channel 406 telemetered the position of relays that controlled the battery charge rate, the status of the relay that automatically transferred the battery charge rate, and that which controlled boosting. Also, telemetry Channels 411 and 434 provided temperature data for PCE Bays I and II, respectively, that housed power subsystem electronics.

j. **MM'71 Power Subsystem Weight.** The MM'71 power subsystem weight was about 106 Kg (165 pounds) excluding associated structures, some 16.78 Kg (37 pounds) heavier than that for MM'69. See Table 1-4. Most of the weight increase was due to the 26 cell NiCd battery that weighed 29.03 Kg (64 pounds) including chassis. The MM'69 Ag-Zn 18 cell battery and chassis weighed 16.78 Kg (37 pounds). Battery cell containers accounted for much of the weight difference. Those for the Ag-Zn cell were made of Cycolac resin that were lighter than the stainless steel containers used in the Ni-Cd. The MM'71 PCE was also heavier, by 4.35 Kg (10 pounds), while the weight of the array was essentially the same.

Table 1-2. Mariner 9 Minimum and Maximum Power Requirements

Typical requirements are shown in Figure 2. Peak load rating for the booster regulator and the 2.4 kHz inverter are 295 and 250 watts respectively.

Mission Phase	Date	Array Load watts	Output Power	
			Booster Regulator w.	2.4 kHz Inverter w.
Minimum Power, Post Launch Cruise	3 June 71	232.8	101.4	87.3
Maximum Power, Solar Array Test No. 1	29 Feb 72	451.0	266.0	237.4

Table 1-3. Mariner Mars 1971 Orbiter Powet Subsystem Telemetry Channels

Telemetry Channel	Function
116	PSL output voltage
203	+X solar panel current
204	+Y solar panel current
205	Battery voltage
206	RFS and de heater current
216	400-Hz inverter input current
221	2.4-kHz inverter output voltage
222	2.4-kHz inverter output current
223	-X solar panel current
224	-Y solar panel current
225	Battery output current
226	Booster regulator input current
229	30-Vdc regulator input current
300	Main 2.4-kHz inverter input current
303	30-Vdc regulator output voltage
305	Battery charger output current
405	Battery temperature
419	+Y solar panel outboard temperature
423	Standard cell voltage
424	Standard cell current
425	Radiation-resistant cell current

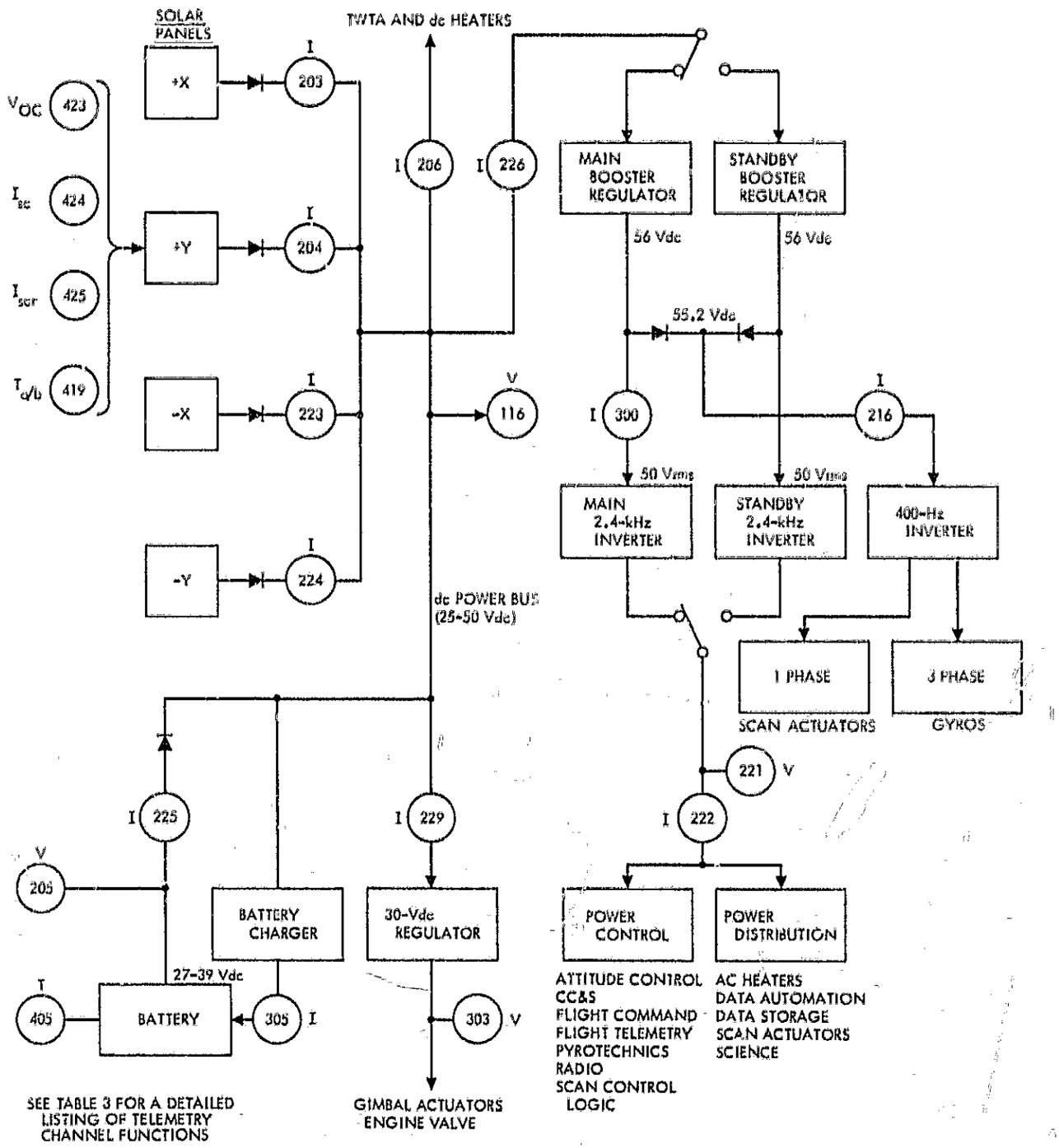

Figure 1-9. MM'71 Simplified Power Subsystem Block Diagram

Table 1-4. MM '71 Power Subsystem Weight, kilograms

Solar Cell Array Assembly, total		24.86		
Solar Panel Strctures (4)			26.49	
Battery, Including Chassis		29.03		
Bay I Electronics Assemblies				
Bay I Chassis			2.38	
Power Source Logic		4.70		
Main Booster Regulator		2.68		
Standby Booster Regulator		2.68		
Power Control		1.09		
Battery Charger		1.41		
	total	12.55		
Bay II Electronics Assemblies				
Bay II Chassis			2.48	
30 Vdc Regulator		1.94		
Power Distribution "A"		1.52		
Power Distribution "B"		0.67		
2.4 Hz Main Inverter		1.30		
2.4 Hz Standby Inverter		1.30		
400 Hz 1 and 3 Inverter		1.61		
	total	8.34		
Total MM'71 Power Subsystem		74.78		
Total MM'71 Power Subsystem Associated Structures			31.35	
Grand Total MM'71 Power Subsystem Weight				106.12

SECTION 2
MARINER 9 FLIGHT PERFORMANCE

2.1 LAUNCH

The Mariner Mars 1971 Orbiter flight performance is the flight performance of Mariner 9, after a Centaur inertial guidance failure caused Mariner 8 to be lost at sea during its launch May 8, 1971. The Mariner 9 battery discharged 8.76 ampere-hours during its launch sequence 30 May 1971. The average discharge rate was 8.1 amperes for a total depth of discharge of about 44%. Other launch parameters during the Mariner 9 launch are shown in Table 2-1 where comparisons are made with those of Mariners 6 and 7. The greater number of cells in the Mariner 9 battery accounts for its higher potential in the Table. After the solar panels deployed during the Mariner 9 launch sequence, an onboard timed command was issued to transfer the charge from low rate to the high charge rate mode. The battery charged at high rate for 3 hours 52 minutes, until the charger voltage detector circuit automatically transferred the charger to the low rate mode. The battery continued to recharge at low rate for an additional 3 hours and 23 minutes. The battery temperature began to rise after this interval that signalled the end of recharge, and the start of the normal battery trickle charge phase. Except for occasions when a direct ground command was used to obtain the high charge rate, this was the pattern for recharging the battery of Mariner 9 for the balance of the mission.

2.2 MARINER 9 CRUISE TO MARS

No battery energy was required to supplement the Mariner 9 solar array power output during the midcourse correction maneuver 4 June 1971. At this stage in the mission, the spacecraft was close to the sun, and the array output power capability was far in excess of the spacecraft power requirement, even with the 44.7 deg turn from the sun required for the proper motor thrust vector. The spacecraft required 301 watts at the array during the maneuver. The array maximum power on the day of the maneuver was estimated at 845 watts with the solar array normal to the sun. It was estimated at 632 watts when the spacecraft was maneuvered from the sun for the motor burn, with the effects included for array shadowing by spacecraft structures.

Performance changes within the Mariner 9 power subsystem were of interest during the cruise to the planet. One change was the gradual potential increase on the dc power bus. With a constant spacecraft power profile, the array operating point gradually increased in potential, as the array temperature slowly declined because of the recession of the spacecraft from the Sun. The dc power bus potentials are plotted in Figure 2-1 along with the Mariner 9 heliocentric distance and array peak power output. The bus voltage and Sun distance curves have similar shape due to the relationship of the array operating point with a given load, the array temperature, and heliocentric distance. The dc power bus voltage increased until the array zener diode circuit activated to clamp the array potential. This occurred on 18 October 1971, 141 days after launch, and 27 days before Mars orbit insertion. The Mariner 9 heliocentric distance at the time was 202.99 $(10)^6$ km, the sun intensity 75.90 mw/cm^2, the array temperature 3.3°C, the array load 303.1 watts, and the dc power bus voltage was 45.4 volts. An average potential curve is drawn through the data points in Figure 2-1, and this curve shifted down when the TWTA was commanded into its high power mode, on 21 August 1971, to cause a 33 watts power increase at the array. Pre-encounter science loads, 66 watts at the array, also shifted the curve downward on 11 November 1971, after the array zeners were limiting.

Battery operation also changed with the Mariner 9 trajectory to Mars. As the dc power bus potential increased, as shown in Figure 2-1, the potential drop across the battery charger increased, as shown in Figure 2-2. After launch, the dc power bus potential was 2.8 volts above the battery potential, the difference between the two being the battery charger potential drop. With this low potential drop, the battery low charge rate was 0.282 amperes. The full limiting low charge rate was 0.614 amperes, but the limiting rate was attained only after the potential drop across the battery

Table 2-1. Mariners 6, 7, and 9 Power Subsystem Launch Performance Compared

Parameter	Mariner		
	6	7	9
Time on battery power, minutes	36.8	59.8	64.9
Maximum battery discharge current, A	10.29	10.27	9.18
Total battery discharge, A-h	8.6	10.6	8.8
Minimum battery potential before Sun acquisition, V	26.68	26.68	31.36
Battery Depth of Discharge, Compared to rated capacity, %	17.2	21.2	44
Minimum bus potential before Sun acquisition, V	25.83	25.84	29.6
Maximum near-Earth bus potential with array operating cold, V	46.98	46.76	46.6
Minimum array temperature in Earth shadow, °C	-2.2[a]	-83.4	-87.8
After 24 hrs of post-launch cruise:			
Primary bus potential, V	39.38	39.58	39.9
Battery potential, V	34.78	34.44	37.5
Total array output current, A	5.82	5.93	5.58
Spacecraft power demand at array, exclusive of battery charger, w	235.7	241.4	228.5
Battery temperature, °C	21.3	22.4	12
Array temperature, °C	55.5	57.5	50.0

[a]Data loss prevented more accurate temperature evaluation.

charger reached or exceeded 5.9 volts. Figure 2-2 shows that the charger low rate gradually increased with the charger potential drop, and that it reached its 0.614 ampere limiting value in steady state on 23 August 1971, 85 days after launch, 83 days before Mars' encounter. During cruise, the battery temperature followed the magnitude of low charge rate. Most of the low rate charge generated heat almost directly proportional to the charge rate level, as displayed in Figure 2-2 by the similarity of the curves for the battery temperature and the trickle charge, as the charge rate changed.

The midcourse correction maneuver caused performance changes in the Mariner 9 battery although it was not used during this mission phase. After reacquiring the Sun, the array operated cold for a short time, and the colder array caused an increased charger potential drop that increased the battery low charge rate. These effects are shown in Figure 2-2. Also shown, are battery temperature increases due to the operation of the propulsion tank heater, and due to the high power TWTA mode. Low rate charger operation was affected by the high power TWTA mode for some days after the event until new equilibrium conditions were reached. The influence upon the low battery charge rate by the potential drop across the battery charger during the mission is shown in Figure 2-3. Battery temperature equilibrium was reached 28 days after launch and lasted over a month. The spacecraft bus temperature then declined starting 65 days after launch because of increased sun distance, and with it, the battery temperature declined. The battery temperature is seen to decrease again for the same reason starting 97 days after launch, after the high TWTA power mode had shifted the battery temperature upward.

Another trajectory related power subsystem change was that of Mariner 9 cruise electrical loads. Although the Mariner cruise power profile changed but once when the TWTA operating mode changed, the total array load increased with heliocentric distance. The array load increase was due to the increasing battery charger power requirements, until it reached its full limiting low charge rate magnitude. It was also due to the increasing dc heater dissipation as the dc power bus potential increased until it became zener clamped. The cruise array load soon after launch was 242.5 watts. It was 255 watts just prior to the pre-encounter science sequences for the identical power profile, ignoring the high power TWTA mode. The 23.5 watt increase represents the influence of the spacecraft heliocentric distance during this interval upon one spacecraft cruise power configuration.

2.3 MARS ENCOUNTER AND ORBITS

Mariner 9 required battery energy to supplement solar array output power during the Mars' orbit insertion phase on 13 November 1971, and again for the orbit trim maneuver No. 1 on 15 November 1971, and the orbit trim No. 2 on 30 December 1971. The spacecraft data record for the MOI is good, but spotty for the trims. Data outages obscured the start and end of the battery discharge sequences for both trim maneuvers. The outages were due to RFS occult intervals because of the planet celestial configuration, and antenna misorientation during the maneuvers. Some battery parameters during the insertion and trim maneuvers are shown in Table 2-2, with estimates where possible.

At encounter, the efficiency of the Mariner 9 solar array solar energy conversion to electrical energy was 11%, about what it was for the Mariner Mars 1969 spacecraft. The Mariner 9 array peak power at encounter is estimated at 512 watts, including 4% array current degradation evaluated from its Isc-Voc transducers.[1] The sun intensity at encounter was 67 mw/cm^2, spacecraft Sun distance 211 $(10)^6$ km, and the array temperature -2.38°C. Also, at time of encounter, the central computer and sequencer clock had gained 15 seconds during the 168 day cruise since launch. The sync pulses for this clock were obtained from the waveshape of the 2.4 kHz inverter output power bus, and the accumulated clock error relates to the accumulated frequency error of the 2.4 kHz inverter.

Routine science recording and playback sequences followed after the successful insertion of Mariner 9 into a Mars 12 hour orbit. The spacecraft operated solely from solar array power without battery assistance for the entire format mission that lasted 135 days until 28 March 1972.

2.4 MARINER 9 EXTENDED MISSION

The extended mission that followed began 29 March and ended 27 October 1972, 212 days later. This mission phase placed the greatest demands upon the Mariner 9 power subsystem. Frequently performed science sequences, formerly supported only by the array, would have to be supported by the battery along with the array

[1] Design and Flight Performance Evaluation of the Mariners 6, 7, and 9 Short Circuit Current, Open-Circuit Voltage Transducers, Robert E. Patterson, November 8, 1972.

Figure 2-1. Mariner 9 Estimated Peak Array Power During Cruise and DC Power Bus Potentials

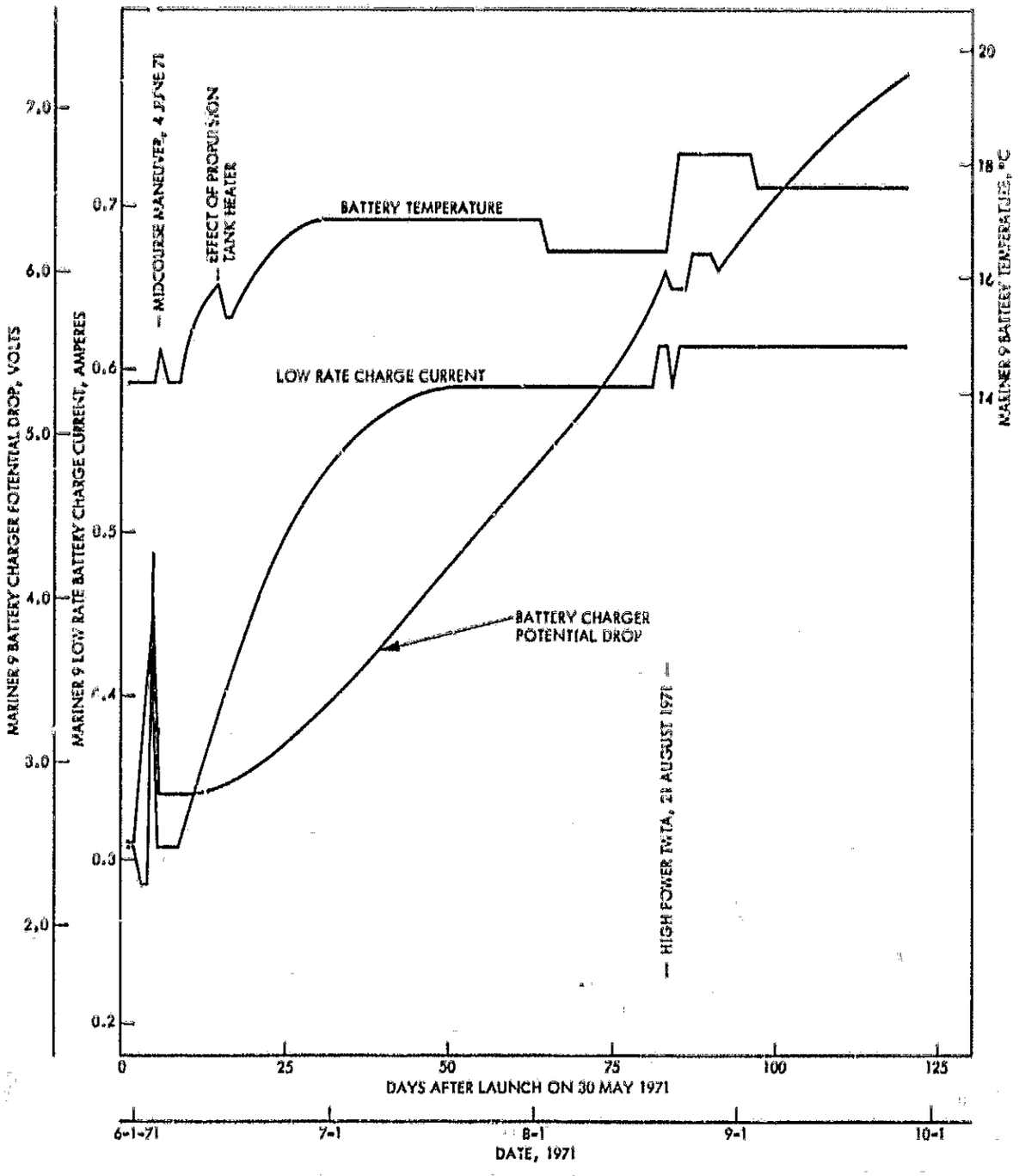

Figure 2-2. Mariner 9 Battery Charge Parameters During Cruise

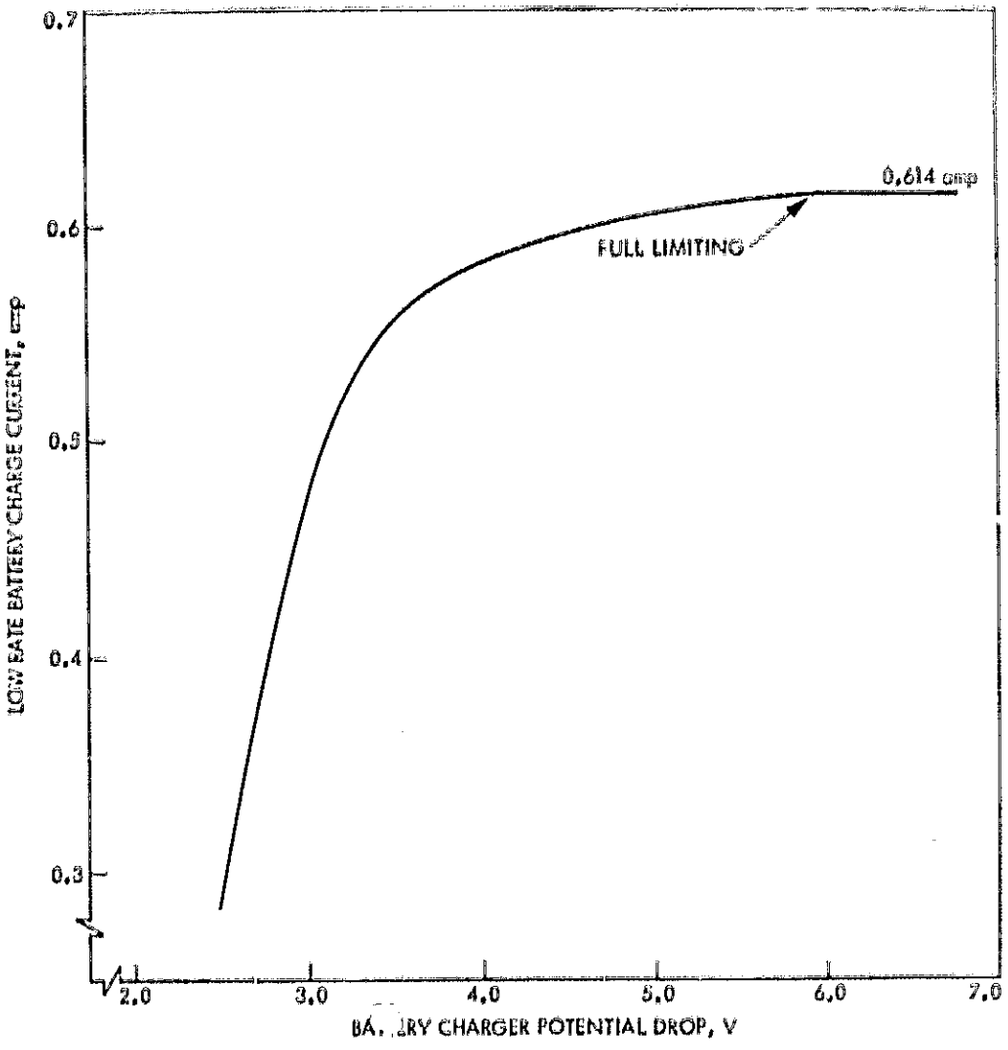

Figure 2-3. Flight Performance of the Mariner 9 Low Rate Battery Charger

Table 2-2. Mariner 9 Battery Performance Parameters for Maneuvers at Mars

	Angle off Sun, deg.	Time on Battery min.	Avg. Battery Dischg Current, a.	Battery Dischg a-h	Recharge at High Chg. Rate		Max. Dischg Temp. °C	Min. Dischg Temp. °C
					Time hrs	Cap. a-h		
MOI	+124.90	40	9.5	6.34	0.4	5.4	20.4	12.5
O/T #1[a]	+128.73	30[b]	9.0[b]	4.4[b]	1.5[b]	4.4[b]	-	-
O/T #2	+118.26	25[b]	9.4[b]	3.9[b]	1.4[b]	4.1[b]	-	-

[b]Estimated

[a]Orbit Trim

as the spacecraft distance to the sun increased. Also, spacecraft to earth distance was increasing too, so that the high gain antenna would have to be used to transmit the science data to tracking stations. This required a high gain antenna maneuver (HGAM) to properly point the antenna to earth for science data transmission. The HGAMs generally caused the solar array to be misoriented from the sun sufficiently to require the battery to share the spacecraft loads with the array. In addition, the battery supported the spacecraft loads during intervals of sun occultations created by trajectory precession in the extended mission that placed Mars between the spacecraft and the Sun for a time during sequential orbits.

The success of the Mariner 9 extended mission was dependent upon the support of the power subsystem, and in many respects, for operations regarding the battery that were used for the first time in this or past Mariner missions. The dominant requirements were proper power management of spacecraft loads and management to attain battery energy balance. Energy balance was achieved with spacecraft operations that were designed to prevent daytime and nighttime spacecraft loads from excessively draining the battery, and designed to provide conditions that permitted adequate battery recharge before the battery was again used.

2.5 POWER MARGIN DIAGRAM

A prime tool for power management was the power margin diagram, one of which, for HGAM's, is shown in Figure 2-4.

A. Use of power margin diagram. The diagram was used to predict occasions the battery would be required to share with the solar array the electrical loads of the spacecraft. It aided the design of specific spacecraft operations on the occasions it was necessary to avoid share during a specific interval, and for the design of other sequences when a share mode was desirable. In addition, operational sequences were studied that required:

1. Boost Pulses. The occasions loads caused battery share when the array was normal to the Sun could also cause futile boost pulses to transfer the power subsystem operating point to the array. Pulses that could interfere with science gathering or playback. The diagram identified these share conditions, that would require either inhibiting boost pulses by command, or prudent reduction of spacecraft loads to avoid share.

2. High Charge Rate. Charging the battery at high rate required about 80 watts, or 33% more array power than the science loads. The diagram aided careful planning for the high rate charge sequences, that may have otherwise caused inadvertent battery discharge instead of charge.

3. Excessive Spacecraft Loads. The diagram revealed occasions when loads would have to be trimmed, and identified load magnitudes to be turned off.

4. Battery Maintenance. It was desirable to routinely discharge the battery moderately during the interval the HGAM's were required, to maintain adequate battery condition that permitted the fullest use of its designed capacity when needed. The power margin diagram again served to indicate when no share was expected, and identified which additional load would provide the desirable discharge. Applying extra spacecraft loads was useful during the early HGAMs when Mariner 9 was maneuvered from the sun to a smaller degree to attain proper antenna pointing to earth. The battery either wasn't expected to discharge because of adequate array margin during these early HGAMs, or it was expected to be discharged lightly.

B. Power margin diagram construction. The diagram assembled a number of parameters to support Mariner 9 power management:

1. Array Output Power. The output power of the array had been estimated based upon ground tests. See section on Mariner 9 Solar Array Performance. The array output predictions were factored for array degradation that had been evaluated from the array Isc-Voc transducers during the mission; and the predictions were further refined with solar array tests.

   a. Orbital Influence. Array output power varied because of array temperature differences at extremes of the orbit. Greater output power was expected at apoapses because of the cooler array, but output power at periapses only was used in the diagram for worst case evaluation.

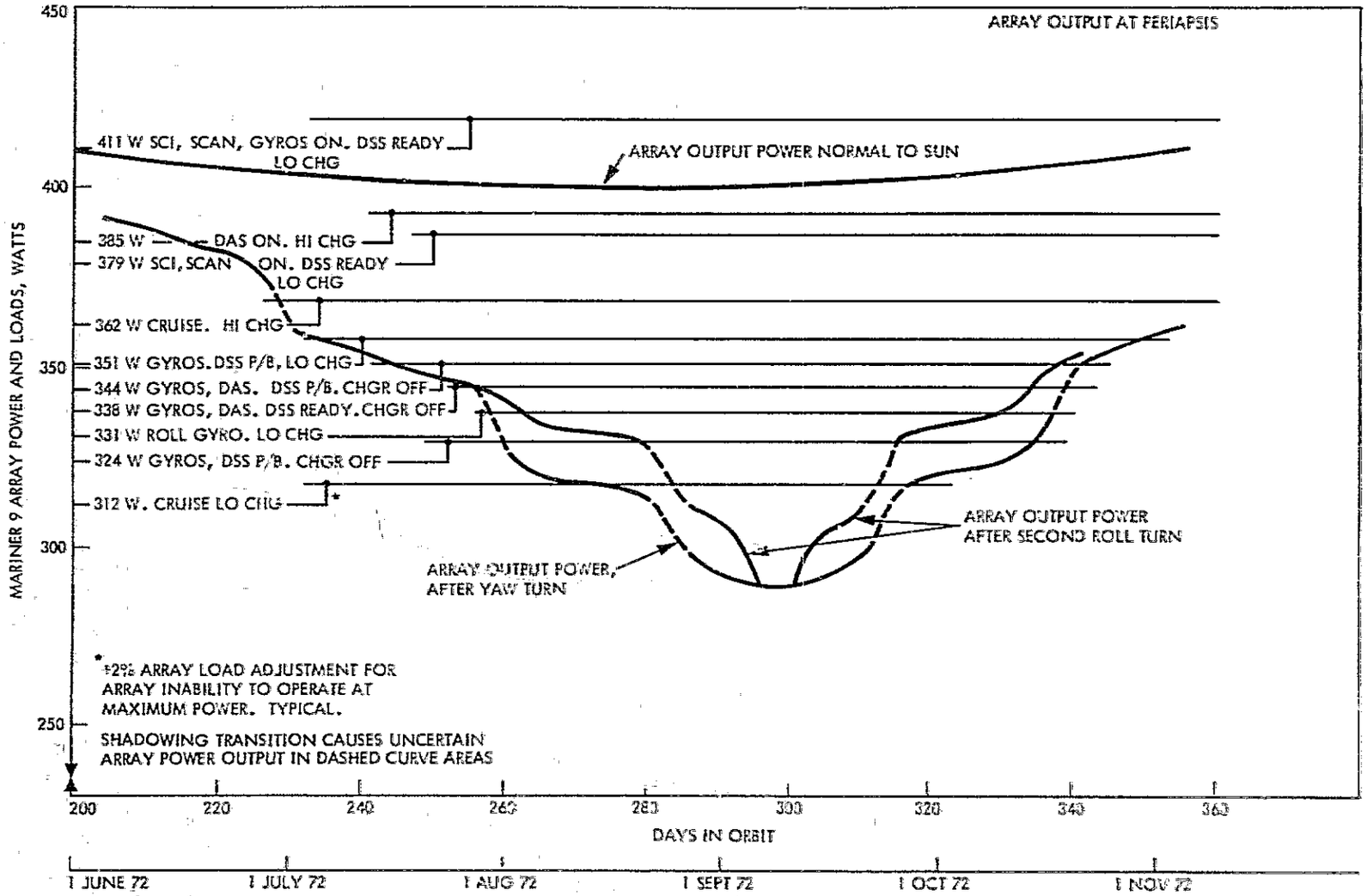

Figure 2-4. Mariner 9 Power Margins During High Gain Antenna Pointing Maneuvers.

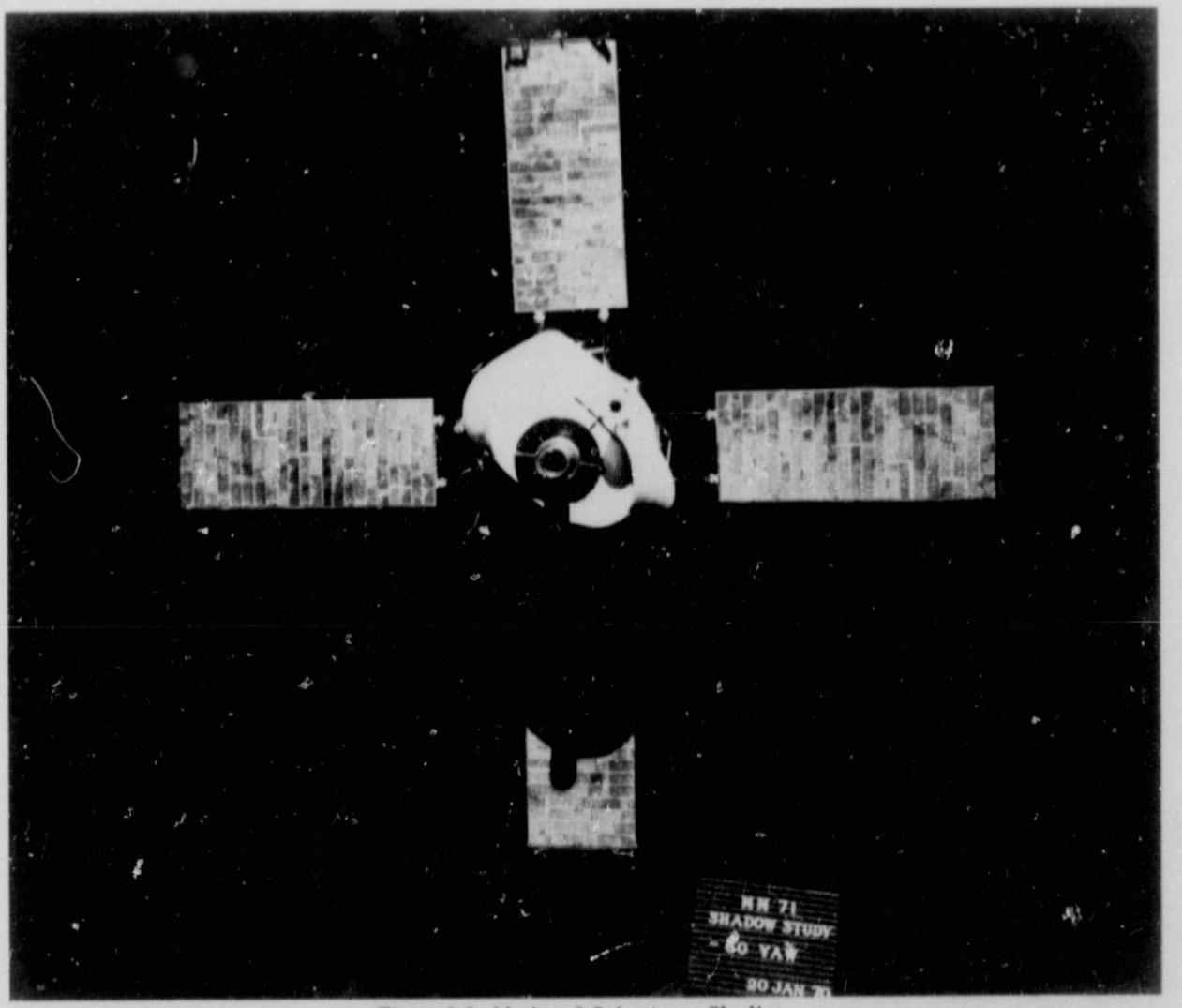

Figure 2-5. Mariner 9 Solar Array Shading

b. Array Orientation. Peak array output as it operated normal to the sun is shown in Figure 2-4 where the minimum array power of 400 watts is seen to occur on 17 August 1972, at the planet's aphelion. The extent the array was misoriented from the Sun to point the high gain antenna to earth was determined by celestial mechanics that depended upon the calendar date, and the resultant array power after these maneuver is also integrated into the diagram. Typical maneuvers had three sequential turns; roll, yaw, and a final roll turn. The initial roll turn didn't affect the array output, but the yaw and final roll turn did, see Array Shading.

c. Array Shading. A sufficiently large yaw turn cast shadows upon the solar panels by low and high gain antennas, the spacecraft bus structure and the solar panel latching devices. Photographs were used to aid the study of the shadow patterns. These were obtained with a Mariner 9 spacecraft model in tests performed in the JPL Celestarium facility. Figure 2-5 shows the array shadow pattern resulting

from a -60 deg yaw turn and 0 deg roll. The study showed significant array shadowing started at a -20 deg yaw. It also indicated that the final roll turn frequently redistributed the shadow pattern to cause some of it to fall between panels, which at times increased the array power output. The array peak power output after the yaw turn required for each date is incorporated into the diagram, as well as the array power increases caused by some of the final roll turns.

d. Array Temperature. Array temperature changed with its Sun orientation and the temperature effects upon the array power output are also integrated into the diagram. Temperature changes because of shadowing were ignored however.

2. Array Loads. A matrix of array loads shown also in Figure 2-4 are of frequently used Mariner 9 power profiles. The loads had been logged from flight data and incorporate the influence of operation on most recently evaluated array zener composite characteristics, the spacecraft hellocentric distance, bus voltage deviations resulting from larger loads, and booster regulator and 2.4 kHz inverter efficiency changes with load. Pre-launch ground test data contributed little to the determination of the manner spacecraft loads influenced the array load, if only because of the poor array-zener composite curve simulation in ground tests. In Figure 2-4, each array load is adjusted by adding 2% to account for ripple power imparted to the dc power bus by the operation of the booster regulator. The adjusted array load more closely resembled the peak spacecraft loads seen at the array.

3. Power Margin. The power subsystem margin is the difference between the array peak power output, and the adjusted array loads during a spacecraft operation. Positive margins could be sustained by the array. Negative margin required battery energy to support the array when operations required spacecraft loads to exceed the array output at a given date in the diagram.

2.6 POWER MANAGEMENT

A. Array Power Estimates Increased. Share modes appeared probable on three occasions during a Mariner 9 HGAM sequence on July 10, 1972. However no share occurred, although the spacecraft telemetry data indicated share to be near on the three occasions. The power margin diagram is not reproduced in this report upon which the share forecast was drawn. The estimated Mariner 9 solar array output in this diagram for the period had been degraded 3.5 percent in current, which was apparent from array Isc-Voc data at the time. The array output in the diagram was revised upward 2.7% on the basis of data received from solar array tests 2 and 3. See section on solar array tests. The revised diagram, Figure 2-4, was issued 20 July 1972, and the first opportunity to test its validity was during a HGAM on 7 August 1972. The following describes the manner in which the accuracy of the diagram was confirmed, and it also illustrates the typical manner the margin diagram was put to use to support the power management of Mariner 9.

B. HGAM of 7 August 1972. The problem of the 7 August HGAM was to have the Mariner 9 power subsystem support a 9.5 hour science playback. With an array load of 368 watts and the array oriented 31.3 deg from the sun, the loads appeared certain to require battery share. Also, it appeared the loads would require the battery to discharge in excess of 18 ampere-hours, its limit in operations during this mission phase. Since most of the recharge sequence that followed occurred without spacecraft telemetry surveillance, the 18 amp-hr limit provided battery energy reserve in the event of an unscheduled need for battery energy when the spacecraft wasn't monitored. As an example, loss of Canopus lock and the resultant automatic roll search could put the battery that possessed a low charge state, into share until a star reference was again regained. The plan was to minimize share during the 9.5 hour interval by discretely removing loads without jeopardizing playback, and the margin diagram was put to use to effectively deal with the problem in the following manner.

C. Margin Diagram Parameters for HGAM. The margin diagram, Figure 2-4, indicated the peak array output on 7 August:

1. would be about 400 watts normal to the Sun. The first roll turn of the roll-yaw-roll maneuver for antenna pointing would not affect peak power.

2. would be 319 watts after the yaw turn, when the spacecraft structures were expected to shadow a portion of two solar panel sections.

3. would be 333 watts after the second roll turn that completed the maneuver. A portion of the array shadow was expected to fall between two panels after the second roll turn, and but one solar panel section was expected to remain somewhat shaded.

D. Managing Power for HGAM

1. Battery Charger. The battery charger was turned off to save about 30 watts at the array, so that the total array load was 368-30 = 338 watts going into the yaw turn on 7 August. During the yaw turn, negative margin, (319-338) ÷ 0.98 = -19 watts, was expected to cause share. Share did occur as predicted. Boost pulses were seen in the data, the consequence of a prior simulated sun gate command, but no successful boost was possible.

2. Data Automation Subsystem. Science data playback began once the maneuver was complete, to point the high gain antenna to earth, and soon after, the DAS could be turned off. This instrument had been on for four days as a timing reference for science data acquisition, and a minimum of ten minutes of played back science data was required to obtain an adequate sampling reference for the DAS B picture timing pulses. Turning DAS off after the ten minute period saved an additional 23 watts at the array, and the margin diagram indicated the resultant power margin would then be 333 - (338-23)/0.98 = +12 watts. Because of the positive margin, and since the simulated sun gate logic had been commanded on, the power subsystem would be expected to immediately boost out of share upon the receipt of the DAS off command. It did during the actual sequence, and array power continued to support the science playback as the spacecraft remained yawed off the sun.

E. Another Check of Margin Diagram.

When the science data playback was completed, the spacecraft was maneuvered to reacquire the sun. The maneuver reversed the order of the turns, so that the first unwind roll turn again shadowed a portion of two panels while the spacecraft was still yawed from the sun vector. This maneuver provided another opportunity to check the accuracy of the diagram, for at this time there would be zero array power margin (319-313/0.98 ≈ 0), and share could again be expected. Share did occur for almost three minutes after the completion of the first roll unwind turn, and lasted until the subsequent yaw unwind turn sufficiently reacquired the sun.

F. HGAM Results.

The battery discharged 0.5 amps-hrs in about 18 minutes during the 7 August HGAM, and the balance of the 9.5 hour science playback was supported by array power as planned.

2.7 BATTERY SUPPORT OF SUN OCCULTATIONS

Mariner 9 began its initial sun occultation sequence 2 April 1972 with a total penumbra pass during which the battery didn't discharge. Early umbra occultations began and ended with a penumbra period as long as 7 minutes. The penumbras lasted about 1.5 minutes for the subsequent occultations. The eclipse period lengthened in duration progressively until a peak of about 98 minutes was reached on 21 April 1972, and then progressively diminished, Figure 2-6. No data was recorded during the peak occultation period because the Apollo 16 Mission had priority for the Deep Space Network support. The longest recorded occultation interval occured during orbit 328 on 25 April 1972, 97 minutes of the 12 hour orbit. Calculations based on telemetry indicated the battery discharged 14.17 ampere-hours in this eclipse, about 70% of rated capacity, and the deepest discharge recorded in the mission. Battery performance because of this occultation is shown in Figure 2-7. The nighttime power profiles were constant, although later dark periods in Figure 2-6 are shown to discharge the battery more than those having similar discharge periods earlier. Battery share during lengthy penumbras of the earlier occultations account for the discharge differences.

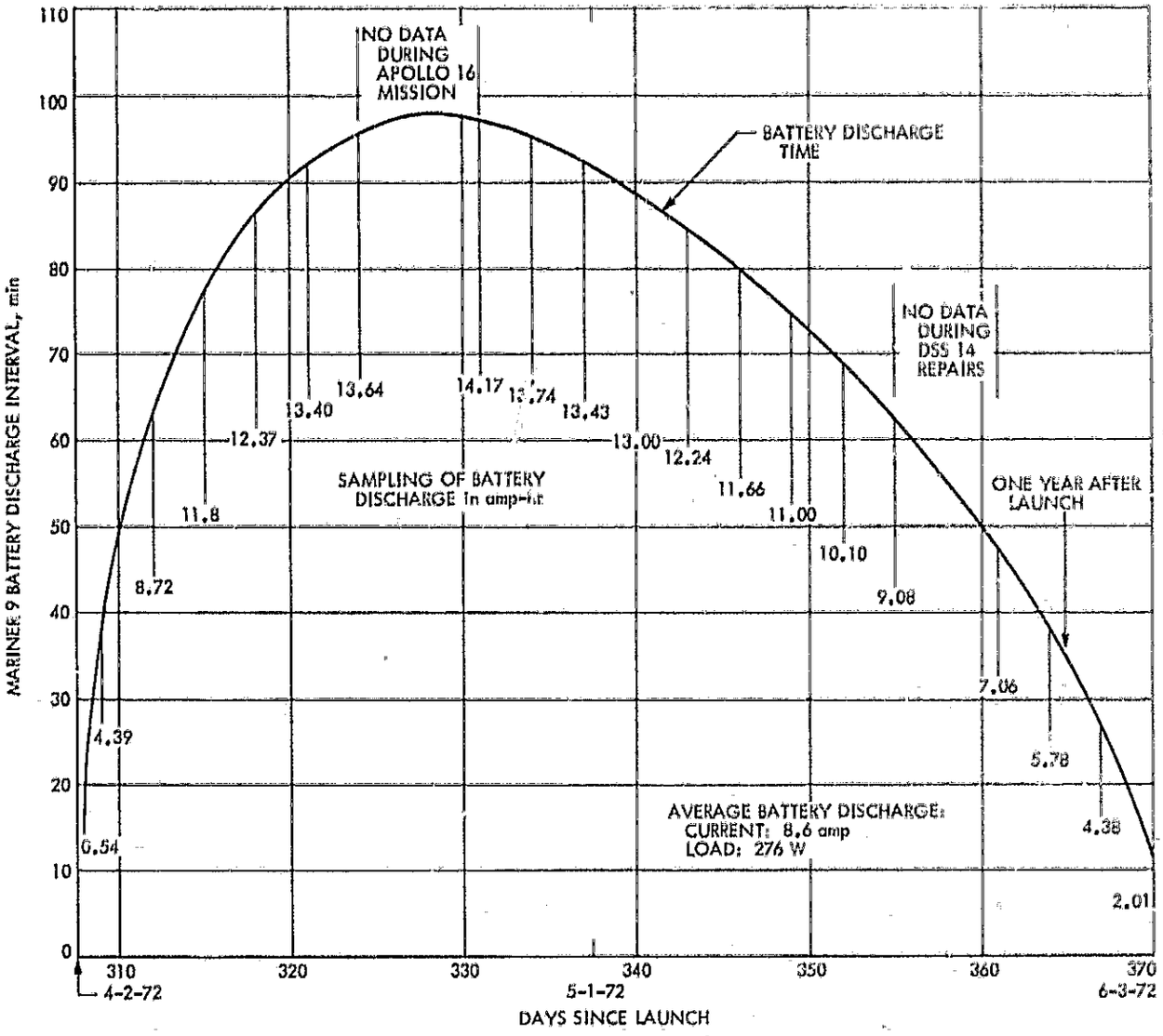

Figure 2-6. Mariner 9 Battery Support During First Occultation Period 2 April to 3 June 1972

The time interval between start of high rate recharge and transfer to low charge rate was empirically derived during the mission, and was repeatedly shown to be accurate, at times within two minutes. The formula:

$$\text{Time to low rate transfer} = \frac{\text{amp-hr dischg} - 1}{2 \text{ amps}} \text{ hours}$$

2.8 CHANGES IN MARINER 9 BATTERY PERFORMANCE

Starting 13 July 1972, 410 days into the mission, the charge potential, in low rate or trickle charge, began a slow decline of 0.8 volts that ended 17 days later. It stabilized at a lower potential (36.39 volts) until the second sun occultation interval, when the battery recovered some of the trickle charge potential loss. The voltage decrease is thought to be the consequence of long term trickle charge, and because of intervals when the battery remained open circuit. The battery charger had been turned off for a number of periods, of up to four days each, because of limited array power near aphelion that was reserved for science gathering sequences. Another apparent change of battery performance occured on 17 October 1972, 506 days after start of the mission, and during a second Sun occultation phase. The battery no longer appeared to follow the empirically derived interval to low rate

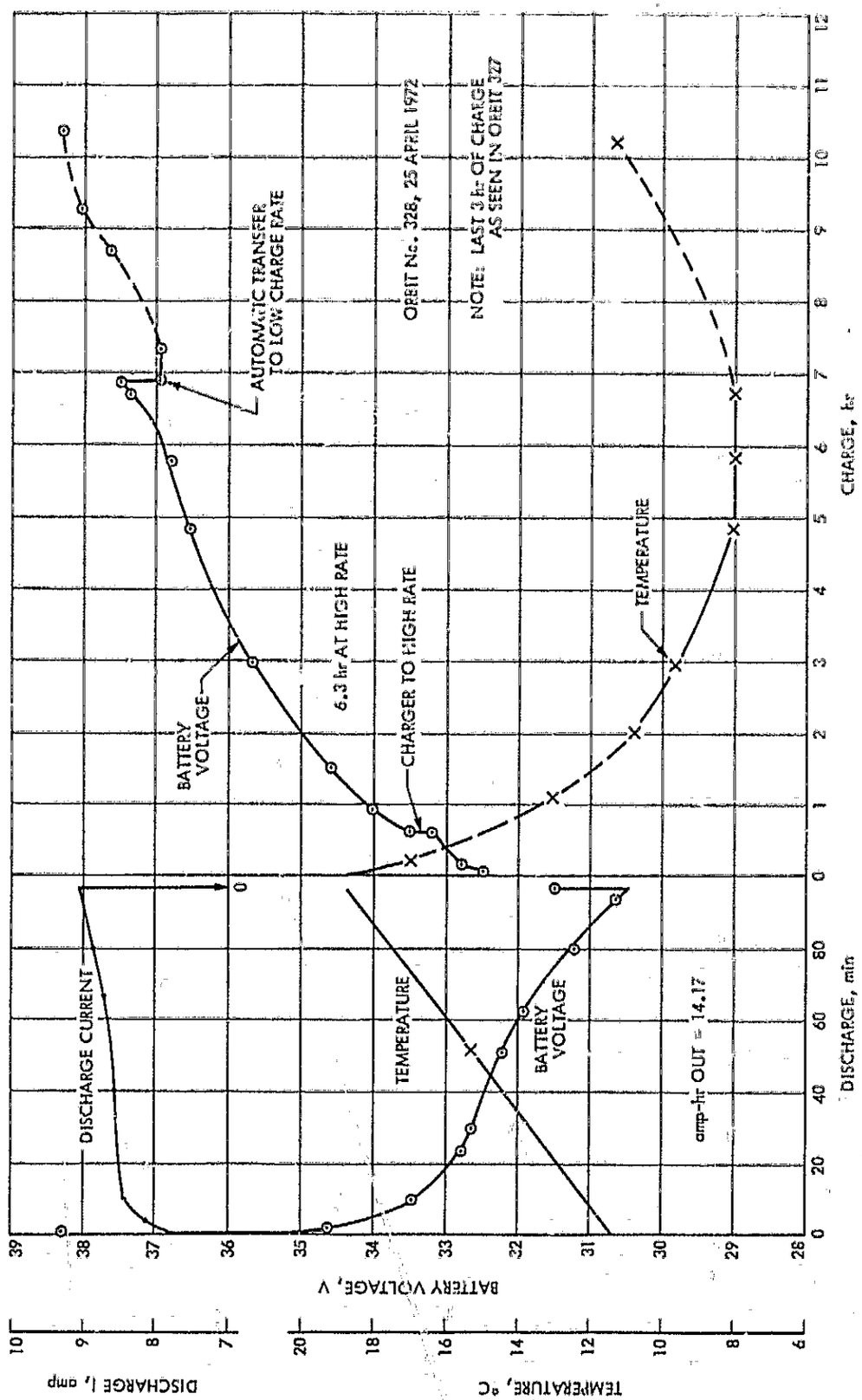

Figure 2-7. Mariner 9 Battery Performance During 97 Minute Sun Occultation Discharge

transfer. The interval to transfer was 57 minutes longer than predicted. Telemetry data doesn't establish reasons for the performance deviations, and both departures from previously established battery performance had no noticeable effect upon the battery's support of spacecraft operations.

2.9 MARINER 9 SOLAR ARRAY PERFORMANCE

A. Array Power Estimates

Estimates of the array performance were based upon prelaunch tests of the solar panels at Table Mountain in the San Gabriel Mountains, California. Panel data obtained in ground tests were for conditions much different from those at which the panel operated in space, and special techniques were employed to extrapolate the Table Mountain data to space conditions.

1. **Solar Cell Standards.** To aid the extrapolation, solar cells typical of those used in the solar panel fabrication were flown at high altitude. They were mounted on special plates, Figure 2-8, and tested at about 36,576 m (120,000 ft) on balloons, Figure 2-9, from which test data was telemetered to earth. At this altitude, the cells were 99.5%[1] above earth's atmosphere where water vapor and ozone bands are absent that significantly alter the Sun's spectra seen on earth. The flown solar cell standards were tested at Table Mountain

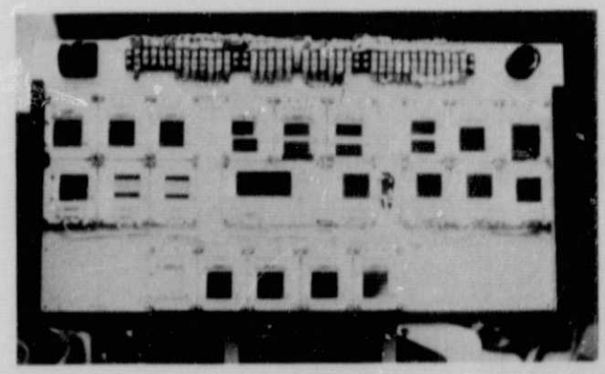

Figure 2-8. Solar Cell Standard Test Panel

along with the solar panels, where a factor was yielded to extrapolate the standard cell ground test data to space performance, when the cells' Table Mountain and balloon performance were compared. Test data reduction of the standard solar cells and solar panels include normalizing to given operating conditions. This extrapolative factor then becomes the key to estimate the solar array flight performance, as it was also applied to extrapolate the Table Mountain solar panel data to space conditions.

2. **Conditions Affecting Array Performance.** Array performance predictions at various mission phases depend upon the estimated array operating conditions at these phases, conditions that change for a number of reasons. They change with spacecraft sun distance because of different sun intensity and array temperature. Array zener characteristics also change with heliocentric distance that influence their junction temperature. Both temperatures also changed within one Mars orbit, with the greatest change occurring at orbit periapses where planetary effects were most pronounced. This was particularly the case during earlier orbits when periapses were near the sub-solar point of the planet. Array data indicated no planetary influence at apoapses. Finally, array performance characteristics also changed as the array degraded.

3. **Array Operating Point.** An array load operates at a discrete operating point on the array-zener composite curve. This operating point on an I-V characteristic of the array is a coordinate point consisting of the total array output current and array voltage, the product of which is the array load in watts. This operating point relocates with changes of array load, moving upward upon the array-zener composite characteristics when greater loads require more array current, and downward with smaller array loads, see Figures 2-10, 2-11, 2-12. Because of the varying array characteristics during the mission, a given array load at different times displayed a different operating point.

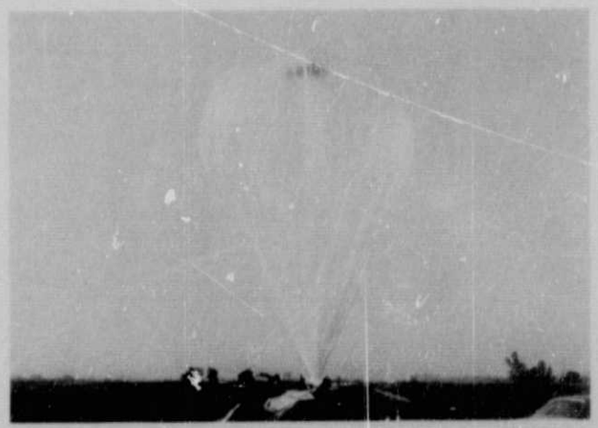

Figure 2-9. Balloons Upon which Mariner 9 Solar Cell Standards were Tested

[1] Results of the 1970 Balloon Flight Solar Cell Standardization Program, R. F. Greenwood and R. L. Mueller, JPL TR 32-1575.

If an assumed array-zener composite characteristic is drawn through the telemetered array operating point on a given day, some measure is conveyed of the array performance. The operating point, however, is just one point on the characteristics. A more accurate assessment requires the array characteristics to be defined by a number of operating points on a given day, which is an introduction to a series of tests conducted on Mariner 9 to confirm its predicted array characteristics.

B. Solar Array Tests

These tests utilized spacecraft loads to vary the array operating point to have resultant telemetry trace the array characteristics. The tests provided a unique opportunity to evaluate the output of a Mariner solar array for the first time in space, and to compare actual with estimated array performance. Test results showed good agreement between the two, actual array peak power deviated less than 3% from that estimated from ground tests data with added estimated array degradation, see Table 2-6.

For each of the four tests, it was possible with load changes to trace the operating point path up the zener characteristics, and to pass its intersection with the array characteristics. But for solar array test (SAT) 2, 3, and 4, array loads were available that were sufficiently large in magnitude on the day of the test to cause the battery to discharge and share the load with the array. The array load causing share is the key to determine the array peak power, but the array peak power in SAT 1

Table 2-3. Mariner 9 Solar Array Test No. 2 Telemetered Data

Point*	Total Array Current, amperes	Array Voltage, volts	Array Load, watts	Battery Discharge Current, amperes	Battery Voltage, volts	Battery Load, watts
1	10.58	32.33	342.0	1.48	33.05	48.9
2	10.58	32.58	344.7	1.48	33.33	49.3
3	10.58	32.83	347.3	1.64	33.61	55.1
4	10.54	32.83	346.0	1.48	33.47	49.5
5	10.58	33.07	349.9	1.64	33.75	55.4
6	10.54	33.32	351.2	1.48	34.02	50.3
7	10.54	33.57	353.8	1.48	34.30	50.8
8	10.54	33.81	356.4	1.32	34.44	45.5
9	10.54	34.06	359.0	1.32	34.72	45.8
10	10.54	34.30	361.5	1.16	35.00	40.6
11	10.54	34.53	363.9	1.16	35.14	40.8
12	10.54	34.79	366.7	1.16	35.42	41.1
13	10.54	35.04	369.3	1.00	35.69	35.7
14	10.54	35.28	371.8	1.00	35.97	36.0
15	10.54	35.53	374.5	0.84	36.53	30.7
16	10.43	39.92	416.4	—	—	—
17	10.38	40.27	418.0	—	—	—
18	10.38	40.52	420.6	—	—	—
19	9.91	43.90	435.0	—	—	—
20	9.90	43.78	433.4	—	—	—
21	9.76	44.25	431.9	—	—	—
22	9.64	44.37	427.7	—	—	—
23	9.55	44.72	427.1	—	—	—
24	9.46	44.72	423.0	—	—	—

*Points are plotted in Figure 2-10.

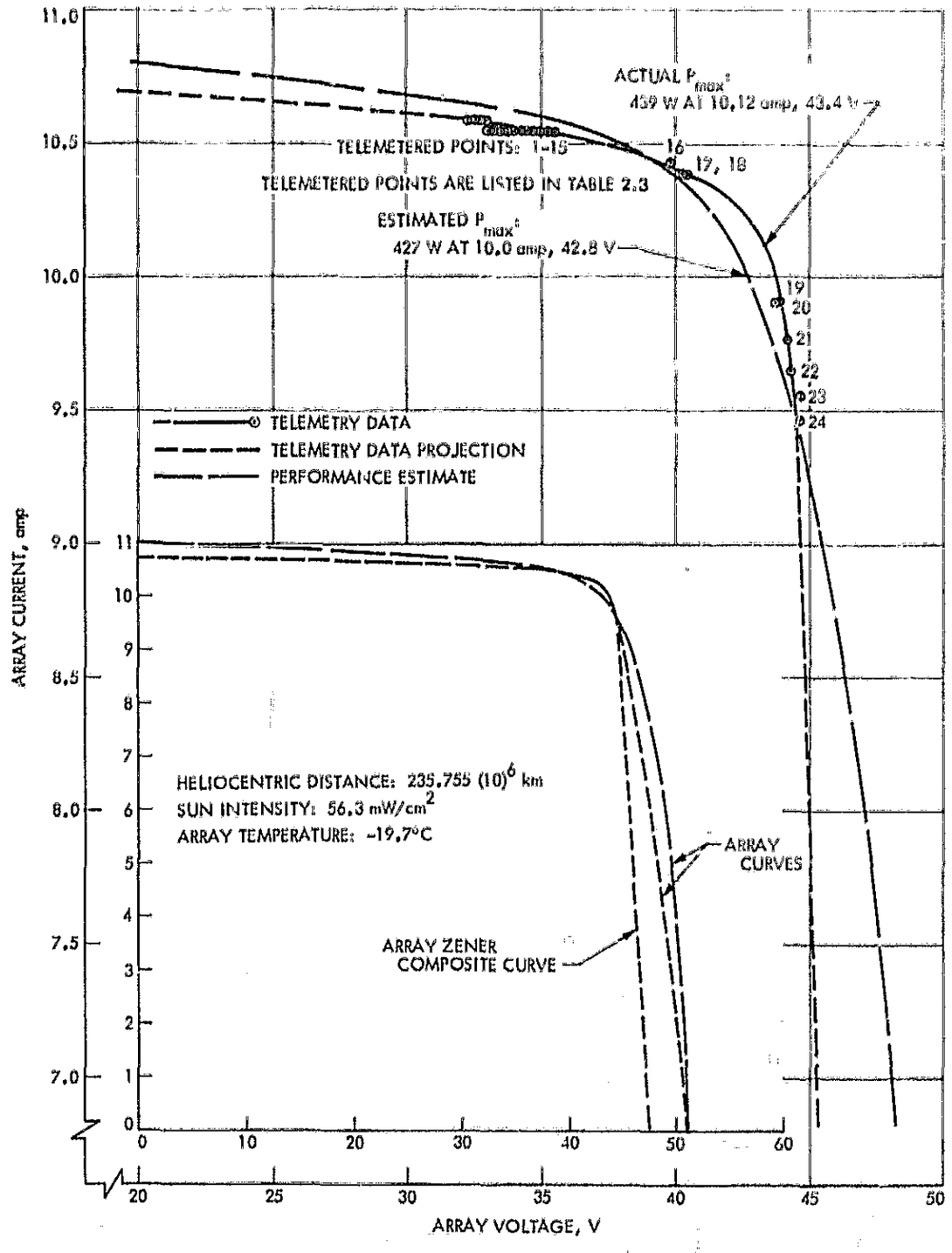

Figure 2-10. Mariner 9 Solar Array Characteristics During Solar Array Test No. 2

Table 2-4. Mariner 9 Solar Array Test No. 3 Telemetered Data

Point*	Total Array Current, amperes	Array Voltage, volts	Array Load, watts	Battery Discharge Current, amperes	Battery Voltage, volts	Battery Load, watts
1	9.68	33.07	319.5	1.48	33.75	50.0
2	9.68	33.32	322.5	1.48	34.02	50.3
3	9.64	33.32	321.2	1.32	34.02	44.9
4	9.64	33.57	323.6	1.32	34.16	45.1
5	9.64	33.81	325.9	1.32	34.41	45.4
6	9.64	34.06	325.3	1.16	34.72	40.3
7	9.64	35.04	337.1	1.00	35.00	35.0
8	8.76	45.45	397.6	—	—	—
9	8.72	45.45	395.8	—	—	—
10	8.60	45.69	392.5	—	—	—
11	8.52	45.69	391.1	—	—	—
12	8.40	45.69	383.4	—	—	—
13	8.20	45.93	376.4	—	—	—
14	7.92	45.93	363.6	—	—	—
15	7.64	46.17	352.7	—	—	—
16	7.60	46.17	350.9	—	—	—
17	7.17	46.17	330.8	—	—	—
18	7.01	46.17	323.5	—	—	—
19	6.97	46.17	321.8	—	—	—
20	6.93	46.17	320.0	—	—	—
21	6.24	46.41	289.6	—	—	—
22	6.20	46.41	288.4	—	—	—

*Points are plotted in Figure 2-11.

was too great for available spacecraft loads to overcome. As the battery discharged in share in the last three tests, its potential declined and generated additional operating points to further define the array characteristic on the short circuit current side of the maximum power point.

SAT No. 1 had been rescheduled to be performed a month sooner than originally planned to confirm the predicted array performance before the first HGAM. The maximum available spacecraft loads for the test totaled 460 watts at the array. Test data indicated an accented array potential decrease when the peak array load was reached, indicating the operating point was near the array maximum power point, but the load was insufficient to reach it. Subsequent array tests were more productive.

1. Array Test Results. Figures 2-10, 2-11, and 2-12 show the estimated Mariner 9 array characteristics as long-dashed curves for SAT 2, 3 and 4 respectively. The estimated curves include 3.5% degradation in array current that appeared to have occurred before the first SAT, and is estimated to have remained constant for the entire series of tests. Estimated curves show only the array characteristics. They do not include estimated zener performance, so as not to crowd the plot of actual data of the array-zener characteristics taken during the tests. A solid curve passes through the array-zener composite curve test data plotted in Figures 2-10, 2-11, and 2-12 tabulated in Tables 2-3, 2-4, and 2-5 for each of the tests.

[1] Mariner 9 Solar Array Design, Manufacture and Performance, E. A. Sequeira, undated.

a. Operating Point Location.

1) With Respect to Zener Operation. The operating point was relatively steady on the zener characteristics. Once the array load increased sufficiently to position the operating point above the zener characteristics, and on to that of the array, the point changed significantly in current and voltage with most telemetry commutations of solar array currents and voltage. The operating point apparent instability was due to activity that was less evident with zener clamp. This activity included de heater cycling, firing of jet valves, subsystem starting transients, and DC power bus ripple imparted by the operation of the booster regulator. The scattered points were cast out in the process of data reduction, since the cause of scatter was understood

2) "Astable" Operation. Points 16, 17 and 18 in Figure 2-10 are unusual operating points that were never before seen during the operation of a Mariner solar array, and which provided valuable insight for the array curve shape. As with operation at the maximum power point of the array characteristics, this operating area was also considered astable, down to the clamping potential of the battery. However, the operating point dwelled

Table 2-5. Mariner 9 Solar Array Test No. 4 Telemetered Data

Point*	Total Array Current amperes	Array Voltage, volts	Array Load, watts	Battery Discharge Current, amperes	Battery Voltage, volts	Battery Load, watts
1	9.32	32.58	303.6	1.96	33.33	65.3
2	9.32	32.70	304.8	1.32	33.33	44.0
3	9.36	32.83	307.3	0.17	33.33	5.7
4	9.32	32.83	306.0	1.64	33.61	55.1
5	9.32	33.07	308.2	1.32	33.75	44.6
6	9.32	33.20	309.4	1.32	33.89	44.7
7	9.32	33.32	310.5	1.64	34.02	55.8
8	9.32	33.57	312.9	1.64	34.30	56.2
9	9.32	33.81	315.1	1.48	34.58	51.2
10	9.32	34.06	317.4	1.48	34.58	51.2
11	9.32	34.30	319.7	1.16	35.00	40.6
12	9.32	34.55	322.0	1.00	35.28	35.3
13	9.32	34.79	324.2	0.84	35.42	29.8
14	8.48	45.21	383.4	—	—	—
15	8.36	45.21	378.0	—	—	—
16	8.36	45.33	370.6	—	—	—
17	8.36	45.45	361.6	—	—	—
18	7.88	45.93	361.9	—	—	—
19	7.44	45.93	341.7	—	—	—
20	7.13	46.17	329.2	—	—	—
21	6.77	46.41	314.2	—	—	—
22	6.74	46.17	311.2	—	—	—
23	6.70	46.17	309.3	—	—	—
24	6.12	46.41	284.0	—	—	—
25	5.36	46.65	250.0	—	—	—
26	5.32	46.65	248.2	—	—	—
27	5.28	46.65	246.3	—	—	—

*Points are plotted in Figure 2-12.

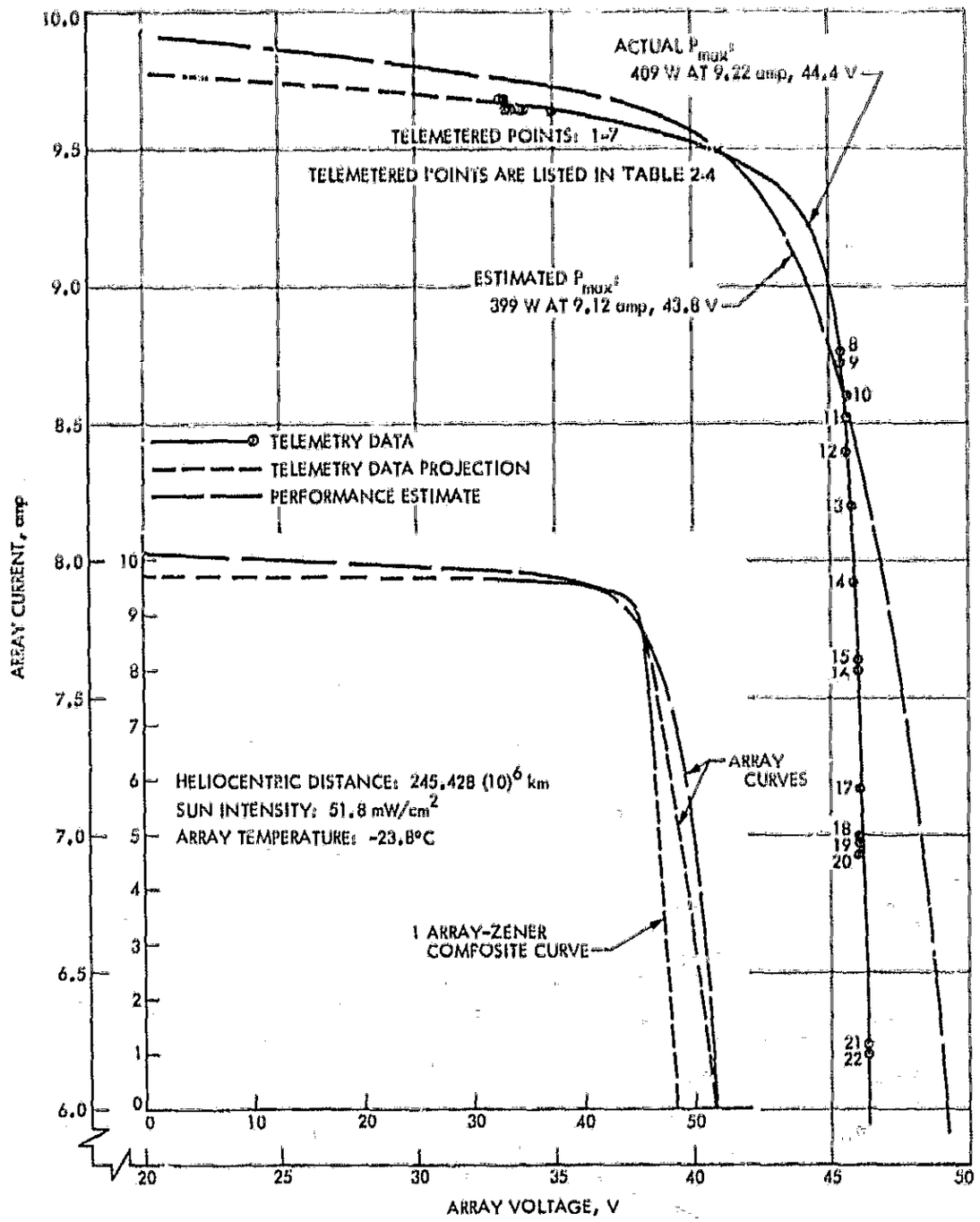

Figure 2-11. Mariner 9 Solar Array Characteristics During Solar Array Test No. 3

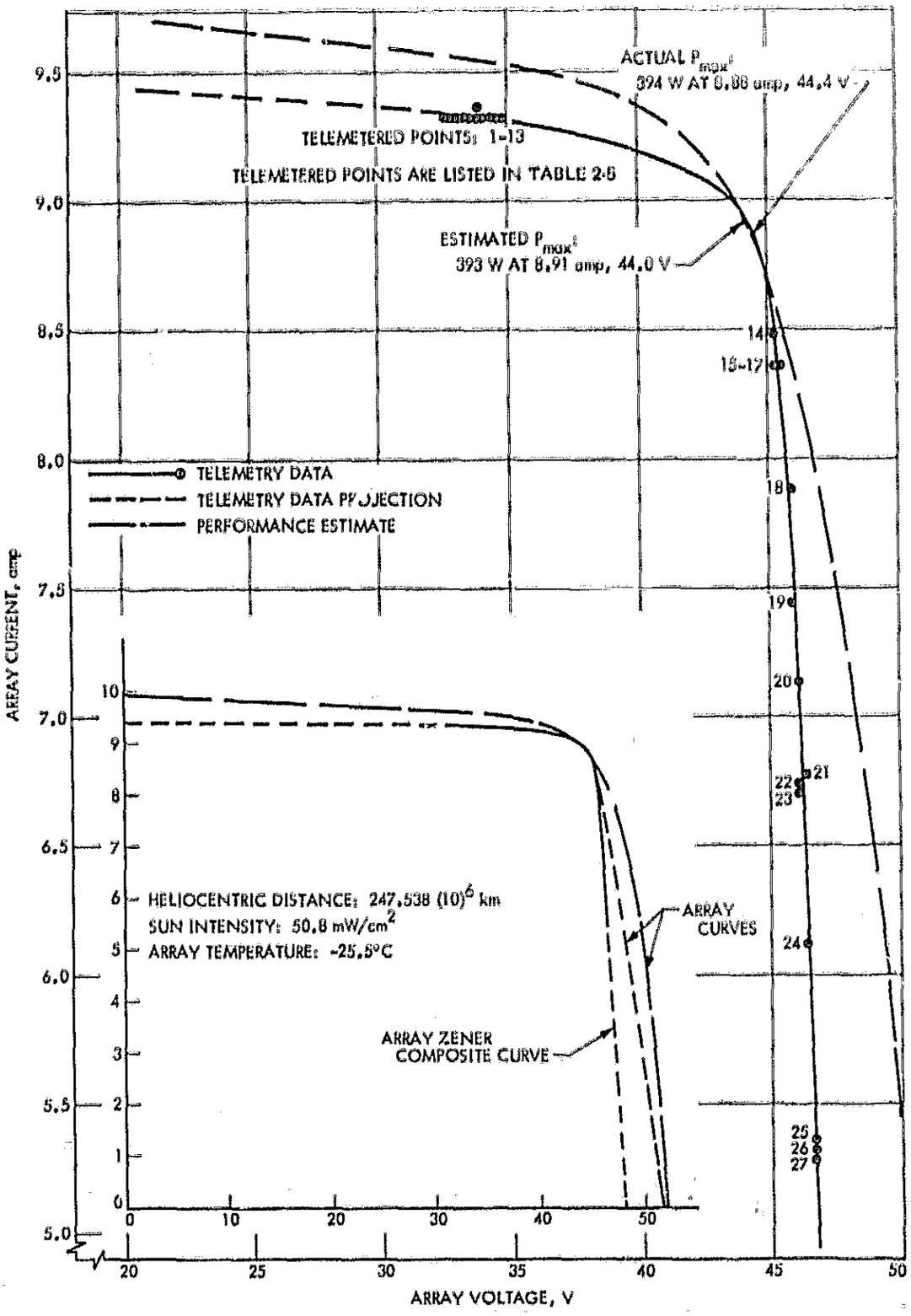

Figure 2-12. Mariner 9 Solar Array Characteristics During Solar Array Test No. 4

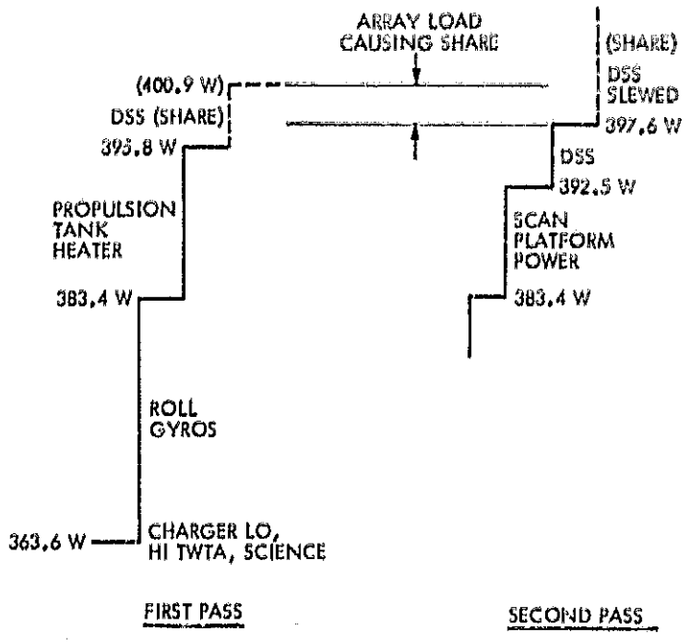

Figure 2-13. Array Load Causing Share in Solar Array Test No. 3

in this "astable" area for 97 seconds during SAT No. 2 to again demonstrate that operation in this area was at least marginally stable, possibly due to automatic array load decrease with declining array potential. The array load apparently reached equilibrium for the short interval at the potential of these points, after the power requirements of the battery charger and dc heaters decreased with array potential. The array had been seen to operate 8 minutes in this area during operations on 11 October 1971, and again for about 10 seconds during SAT No. 4, and for shorter intervals during some spacecraft operations.

b. Maximum Power Point Determination. The maximum power point of the characteristics is not a directly determined telemetered operating point during the tests, since it isn't possible to operate at the maximum power point. Its magnitude was determined indirectly with the magnitude of the array load required to attain the share condition. A series of commanded load increases during the test build the operating points toward peak array power, and share was caused when the array loads exceeded the array peak power. In the test sequence, the smallest loads were reserved for the end of the series to obtain good resolution for that array load causing share. Resolution was then improved by causing share once again with a slightly different series of loads. The load series changed with each SAT because of changes in the array characteristics. Figure 2-13 illustrates the method with the two load series used in SAT No. 3. After the array load was brought to 395.8 watts without share during the first array loading pass in SAT No. 3, share was obtained when the 5.1 watt data storage subsystem was turned on. The array load causing share, therefore, was between 395.8 watts and 400.9 watts, from this series. However, the next array loading series got to 397.6 watts without causing share. Accordingly, the array load causing share lay between 397.6 and 400.9 watts. For SAT No. 2 the load was between 424.2 and 429.8 watts, and for SAT No. 4, between 383.4 and 385.4 watts. Internal to the power subsystem there is an additional load seen by the array. This is the power ripple on the dc power bus because of the operation of the booster regulator. To compensate for the effects of ripple power, two percent of the array load was added to the load to more closely approximate the maximum load seen by the array that caused the share condition.

2. Mariner 9 Solar Array Test Conclusions

a. Solar occultations caused no array degradation

SAT No. 2 was performed just before the start of 124 solar occultations that is estimated to have caused the array temperature to fall as low as -157.8 deg C (-252 deg F) during the worst case eclipse period. It was possible that these array temperature excursions could cause array degradation, but SAT No. 3, that was performed at the end of the sun occultation period, disclosed little evidence of array degradation. Table 2-6 summarizes the maximum array power points and magnitudes obtained from the tests, and the deviations from the estimated magnitudes. From SAT No. 2 data, it shows the array to possess a maximum power 2.8% greater than estimated on the test day, and 2.5% greater after SAT No. 3. The 0.3% decline is not thought to indicate meaningful degradation.

b. Last SAT Indicates Degradation

However, a significant array peak power decrease did occur between SAT 3 and 4 over a period of 119 days. It declined from 2.5% above estimate to 0.2% above estimate, Table 2-6. Apparent array degradation may be due to the unusual solar flare activity the first and second week of August, 1972. These were among the most intense ever recorded at earth. Low energy proton flux of sufficient magnitude at Mars may have caused some array damage. To reach Mars, the flux would have had to be emitted from solar flares sourced at areas of the sun unseen from earth. Although unexpected during the Mariner 9 Mission, the SAT 4 data also appear to indicate that the zeners intersected the array curve on the short circuit side of the maximum power point of the array. If this occurred, it would effectively reduce available array power, and could also account for the array power testing at lower magnitude without array degradation. It may be both reasons. Radiation damage may have reduced array power sufficiently to cause the zener curve to intersect the array curve in this manner.

c. Mariner 9 Array I-V Curve Shape

1) Data Confidence vs Curve Shape. Array output power magnitude varied with the spacecraft heliocentric distance, but the shape of the I-V curve describing the array characteristics was expected to remain unchanged for a normally operating array. Estimated array I-V characteristics possessed the same shape for each SAT, and curves drawn through the test data points for SATs 2, 3 and 4 also had the same shape. This fact further reinforced confidence in the data. The results of the 7 August 1972 HGAM, discussed in Section 2.6, had already demonstrated the reliability of the flight solar array performance data obtained during SAT 2 and 3. Only a

Table 2-6. Array Maximum Power Points Determined by Mariner 9 Solar Array Tests (SAT)

SAT	Date 1972	Mariner 9 Array Maximum Power Point						
		Array Current, a		Array Voltage, v		Array Power, watts		
		Estimated	Actual	Estimated	Actual	Estimated	Actual	% Deviation from Estimates
1	29 Feb	10.34	-	43.4	-	449	460*	+2.4*
2	29 Mar	10.00	10.12	42.8	43.4	427	439	+2.8
3	5 Jun	9.12	9.22	43.8	44.4	399	409	+2.5
4	2 Oct	8.91	8.88	44.1	44.4	393	394	+0.2

*Maximum array load, maximum array capability not evaluated.

small portion of the array I-V curve was obtained in SAT No. 1, and it is omitted from this report.

2) Estimated vs Actual Curve Shapes. Table 2-6 shows estimated maximum power points to be almost 3% less than that obtained in SATs 2 and 3. Figures 2-10, 2-11 and 2-12 show estimates of the short circuit current to be greater than actual, and this portion of the curve was estimated to have had greater slope than displayed in the test data. The actual zener portion of the I-V curves were near estimates.

d. Other Conclusions

The effort to explore as much as possible of the array characteristics by increasing and decreasing loads provided an opportunity to investigate the mechanism of getting into and out of share. Similar tests on ground using the solar array would be futile because of the inability to duplicate conditions of space, and would be futile without the array because of inadequate simulation of the array-zener composite characteristics.

1) Spontaneous Share Transfer. After the battery was sharing the spacecraft load with the array in SAT 3, spacecraft loads were sequentially turned off. The boost converter unit was deliberately inhibited. The goal was to determine to what extent below the array maximum power level the array loads must be reduced to permit the system to transfer from the share mode to operations solely on the array without boost converter pulses. Spontaneous transfer was theoretically possible, and demonstrated during ground tests but with inadequate test conditions. It was never before tested in space. Spacecraft loads were reduced a total of 84 watts below the array Pmax before the next load reduction of 8 watts spontaneously transferred the operating point. The array loads that caused transfer directly relates to the relative battery and array characteristics at the time of the test.

2) Boost Converter Preventing Share. Also in SAT 2, as might be expected, the system went into immediate share when the adjusted array load equaled the maximum power point of the array. The boost converter was inhibited at the time. However, an unsuspected delicate balance was revealed under the conditions of SAT 2, when the boost converter was enabled with the same load profile, and the operating point boosted immediately out of share.

2.10 POWER SUBSYSTEM ASSISTS

The Mariner 9 power subsystem aided in the detection and solution of a number of investigations during the mission. Some of these:

A. IRIS DC Heater Duty Cycling. The MM'71 Infrared Interferometer Spectrometer Subsystem (IRIS) possessed two thermostatically controlled dc heaters, one for its optics, and one for the black body unit. After launch, the optics' heater duty cycle was about 84% on, and that of the black body heater was 100% on. It was a two cycle pattern with the optics' heater cycling on and off. Starting 23 days after launch, the dc heater cycle pattern changed abruptly to four levels. Investigation by the power subsystem showed the black body heater to be cycling, and that the four levels indicated either the black body heater was on alone, or that the optics heater was on alone, or both were on, or off. About 45 days had been expected to elapse after launch before the black body heater cycled.

B. Scan Platform Hit Stop. On 29 November 1971, the scan platform was inadvertently driven into its lower mechanical stop along its cone axis, and held there for about one hour. The sequence was caused by a command processor inadvertently being set into its calibrate position as commands were issued to the spacecraft to have the platform move away from its stop. These commands were not received by the spacecraft, but subsequent commands moving the platform in the direction toward the stop were received, causing the problem. The stop was

hit during an RFS blackout period lasting 35 minutes as the spacecraft moved into a portion of its trajectory that passed behind Mars out of earth's view. It is assumed the clutch slipped until its slip torque increased sufficiently to stall the motor, a desired fail-safe condition. The two watt decrease in scan motor power seen by the power subsystem, as the platform was moved from the stop position, appeared to confirm the stall condition had been achieved. No platform positioning damage or degradation was observed afterwards.

C. TWTA No. 2 Failure. The Mariner 9 power subsystem also contributed to the selection of one of a number of candidate model failure modes of the TWTA No. 2 unit. This unit failed 7 December 1971, again as the spacecraft was in RFS occultation. It had entered occultation performing normally, but exited performing anomalously in a number of ways. Among these were that the RFS electronics bay temperature was increasing, and that the power subsystem noted the dc input power to the TWTA had increased 24.2 watts. It was primarily upon the input power increase to the TWTA that TWTA cathode movement toward the TWTA anode was selected as the most likely failure mode. This movement was thought possible if a weld had broken in one leg of the tripod cathode support structure in the travelling wave tube.

2.11 END OF MISSION

Mariner 9 entered into a second series of sun occultations starting on 5 October 1972, and extending to March, 1973. Eclipses were all about 20 minutes in duration, and to a large extent occurred simultaneously with RFS occultations that severely limited engineering data acquisition. The Mariner 9 battery had supported 38 occultations of the latest series when the attitude control gas depleted on 27 October 1972. The mission ended after 516 days with the exhaustion of this gas supply. During the total mission, the Mariner 9 battery discharged 176 times. A summary of the spacecraft battery activity is shown in Table 2-7. Total accumulated CC&S clock error to the last day of the mission was +57.5 seconds, which approximates the total net frequency error of the 2.4 kHz inverter during the 516 day mission having 12,379 operating hours.

2.12 MM'71 PROBLEM/FAILURE REPORTS

Mariner Mars 1971 power subsystem PFR's are summarized in Table 12. The summary shows a total of 57 were written for MM'71 vs 64 for MM'69. Over 50% of the MM'71 PFR's regarded problems in testing hardware, compared to but 25% in MM'69. Although there were more than twice the component failures on MM'71 than MM'69, there were almost one-fourth the PFR's that required major redesign. Accidental component damage or stress, and PFR's having unknown causes, were about the same for both programs. The PFR numbers noted in the table refer to PFR's on file in the spacecraft reliability section at JPL.

2.13 RECOMMENDATIONS

The following are recommendations that may prove useful for future spacecraft design.

1. Battery Charger Design.

   a. Charger Operation. The MM'71 battery charger design was susceptible to undesirable modes of operation that were the basis of a number of PFR's written during the ground test phase. Undesired transfers occurred from high to low rate charge mode, and internal logic at times prevented desirable transfers. Spacecraft operations during the mission were constrained, and extra commands were required on occasion to prevent the charger logic from locking in high rate, and possibly jeopardizing the battery. The recommendation here is that undesirable side effects of charger operation be thoroughly probed and corrected before design freeze. It should be noted that the idiosyncrasies were well understood, and that simple command procedures could correct a lockup state had it occurred.

   b. Charger Potential Drop Required For Full Charge Rate. The battery charger in low rate mode didn't attain its limiting low charge rate of 0.614 amps until 85 days of the mission had elapsed, and until the potential across

Table 2-7. Mariner 9 Battery Cycle History. The battery discharged 176 times during the total mission.

Mariner 9 Event	Date	Discharge, ah
Launch	30 May 1971	8.76
Midcourse Maneuver	4 June	None
Mars Orbit Insertion	13 November	6.34
Orbit Trim No. 1	15 November	4.4
Orbit Trim No. 2	31 December	3.9*
Solar Array Test No. 2	29 March 1972	4.32
Solar Occultation Sequence No. 1 (124 cycles)	2 Apr to 3 June	14.17 (peak)
HGAM plus Solar Array Test No. 3	5 June	4.30
High Gain Antenna Maneuver (HGAM)	12 June	1.3
HGAM	16 June	1.6
HGAM	19 June	1.6
HGAM	23 June	4.47
HGAM	26 June	4.77
HGAM	30 June	6.68
HGAM	7 August	0.5
Solar Array Test No. 4	2 October	3.39
Solar Occultation Sequence No. 2 (38 cycles)	5 Oct to 27 Oct[a]	3.9*

*Estimated

[a]Last day of mission, depletion of attitude control gas supply.

the charger rose to 5.9 volts. A more desirable design would have effective voltage drop across the charger to achieve full charge rate reduced to a much smaller potential. Trickle charge would then be effective earlier in the mission. More importantly, a difficult array design tradeoff would be simplified for the solar cell series vs parallel arrangement with a decreased potential drop requirement across the charger. The tradeoff regards charging the battery near earth, array output power at Mars, and also array potential at Mars.

The series length of the solar cells in the array design is largely determined by the charger potential drop requirement during the near-earth phase of the mission, when the array operates warm. The array operating potential is lower when it's warm, so that the series length of the solar cells must be increased to accommodate the needs of the charger. Operating colder near Mars, the increased solar cell series length serves to raise the array potential too high. It is then limited by the array zeners to potentials used by the system. See recommendation for array

Table 2-8. Mariner Mars 1971 PFR Summary

	Component Failure	Caused Redesign	Component Damaged or Stressed Accidently	Manufacturing	Specification Problems	Test Problems			Unscreened Component Failures (Prototype)	Unknown Cause	Totals	
						Equipment	Facility	Procedures			MM'71	MM'69
Power Conditioning Equipment	104311	103614	103607	103417	104309	103724	103415	103409	104302	103481		
	104312	103680	103612	103628		104301	103495	103500		105493		
	104313	103681	103677	104314		104303		103710				
	104319		104307	104316		104304		103719				
						104305		103720			37	44
						104308		104317				
						104318		105302				
								105316				
								105323				
Battery					104373	102391		103798	103619	105518		
					104374	104369		104362				
					104375	104371		104363				
					104376			104364				
								104365			18	11
								104366				
								104367				
								104370				
								104372				
Solar Array	104315								2	103475	2	0
MM'71 No.:	5	3	4	4	5	10	2	18	2	4	57	
MM'71 %:	9	5	7	7	9	18	3	32	3	7	100	
MM'69 No.:	2	11	4	16	7	8	2	6	3	5		64
MM'69 %:	3	17	6	25	11	13	3	9	5	8		100

zener diode design below. Zeners limited the array potential about a month before Mars encounter, and virtually the entire mission thereafter, during the missions of Mariners 6, 7 and 9.

Decreased charger potential drop for charge rate limiting, decreases the number of solar cells required in series near earth, and could permit instead additional parallel solar cell strings to be incorporated into the given solar panel area. Increased number of parallel strings increases the available array power at Mars, which is the most favorable design tradeoff.

2. Array Zener Diodes. The array zeners started limiting 27 days prior to Mars encounter, at a dc power bus potential of 45.4 volts. The zener circuit serves to limit the input potential to the booster regulator below that of the regulator output of 56 volts, since the regulator isn't designed to operate at input potentials higher than its output. But perhaps the zener circuit needn't be designed to limit the dc power bus at so low a potential, and have it still meet the booster regulator design requirements to maintain loop stability. If the zener cutoff potential could be raised:

   a. Zener Dependence. The time zeners limit would be reduced in the mission, since the time they limit would be delayed and the time they cease limiting would be advanced. Zener current densities would also diminish at given heliocentric distances. Thus raising the zener cutoff potential would be in consonance with sound design for space application to reduce to a minimum current carrying paths and current densities.

   b. Clipping Array Maximum Power. There is telemetry evidence indicating that the zener diode characteristics intersected the array characteristics on the short circuit current side of the array maximum power point for a two month period near aphelion. Maximum power point clipping in this manner means the zener characteristics effectively reduced the array power output for the spacecraft during this interval, and a review of the array zener circuit design could prevent this occurring in future spacecraft.

3. Solar Array Power vs Spacecraft Loads. Science gathering was brought to a halt during the sun occultation phases. The spacecraft loads and solar array should be so sized as to permit simultaneous operation of the high rate charger and science, so that science data retrieval could be extended.

4. Effects of Boosting. Much effort was expended to avoid science recording or playback sequences at times boost pulses may have occurred. It was suspected the boost pulses may have interfered, but this never was confirmed during the mission since the penalty was possible data loss. Boost pulses prevented DAS timing pulses from incrementing properly during the mission, however. No formal investigation of possible interference was performed during ground tests, a lapse that should be remedied in future programs.

5. Load Tests. Each flight spacecraft should have documented in the spacecraft assembly facility the measured power requirement of each subsystem, in the most frequent operating modes. This would better enable the power subsystem to confirm proper operation, and to record possible drift in power requirements during the mission. This data record was completed in MM'69, but only the PTM was so tested in MM'71.

6. Antenna Orientation. High gain antenna articulation design attaining greater orientation capability in future designs would eliminate much of the maneuvering, gas consumption, and the power management that attended high gain antenna pointing maneuvers in MM'71.

7. Emergency Commands

a. Celestial Reacquisition. The emergency reacquisition command on MM'71, DC-13, was associated with the possibility of a single failure that could halt the mission. The command initiates reacquisition of Canopus and the Sun should a problem occur during a maneuver. If the failure occurred, no future maneuvers could be performed. An emergency command of this nature is a requirement on a spacecraft. From the power subsystem view, it could efficiently terminate a maneuver, which for some unexpected reason is critically draining the battery. However, a command of this nature should be designed free of prospects of additional critical spacecraft problems if used.

b. Power Profile Restoration. The mechanization of one command would be valuable in future missions that could be issued to the CCS to restore the spacecraft power profile to a preselected power configuration. One such command would have been useful on September 27, 1972 when the first attempt for SAT No. 4 was aborted. The boost converter was inhibited, and the DAS and IRIS had been commanded on to start the test when a DSN 14 transmitter power supply broke down. This left the spacecraft vulnerable for hours to possible loss, until reconfigured by individual commands from another station some time later. Repetitive issuance of one command to the CC&S would have been more efficient.

8. Solar Array Calibration. Future missions should have as standard operating procedure, tests to confirm solar array performance predictions.

9. Telemetry Voltage Standard. There is always a question regarding the spacecraft power profile, whether some change may be due to drift in some potential level in the spacecraft telemetry subsystem. A voltage standard routinely commutated and telemetered could add confidence to data obtained over long intervals.

10. International Units. Temperature telemetry should be calibrated in °C rather than °F.

NASA — JPL — Coml., L.A., Calif.